REPORT No. 820

PROPELLERS IN YAW

By Herbert S. Ribner

SUMMARY

It was realized as early as 1909 that a propeller in yaw develops a side force like that of a fin. In 1917, R. G. Harris expressed this force in terms of the torque coefficient for the unyawed propeller. Of several attempts to express the side force directly in terms of the shape of the blades, however, none has been completely satisfactory. An analysis that incorporates induction effects not adequately covered in previous work and that gives good agreement with experiment over a wide range of operating conditions is presented herein. The present analysis shows that the fin analogy may be extended to the form of the side-force expression and that the effective fin area may be taken as the projected side area of the propeller. The effective aspect ratio is of the order of 8 and the appropriate dynamic pressure is roughly that at the propeller disk as augmented by the inflow. The variation of the inflow velocity, for a fixed-pitch propeller, accounts for most of the variation of side force with advance-diameter ratio V/nD.

The propeller forces due to an angular velocity of pitch are also analyzed and are shown to be very small for the pitching velocities that may actually be realized in maneuvers, with the exception of the spin.

Further conclusions are: A dual-rotating propeller in yaw develops up to one-third more side force than a single-rotating propeller. A yawed single-rotating propeller experiences a pitching moment in addition to the side force. The pitching moment is of the order of the moment produced by a force equal to the side force, acting at the end of a lever arm equal to the propeller radius. This cross-coupling between pitch and yaw is small but possibly not negligible.

The formulas for propellers in yaw derived herein (with the exception of the compressibility correction) and a series of charts of the side-force derivative calculated therefrom have been presented without derivation in an earlier report.

INTRODUCTION

The effect of power on the stability and control of aircraft is becoming of greater importance with increase in engine output and propeller solidity. An important part of this effect is due to the aerodynamic forces experienced by the propeller under any deviation from uniform flight parallel to the thrust axis. The remaining part is due to the interference between the propeller slipstream and the other parts of the airplane structure.

A number of workers have considered the forces experienced by the propeller. It was pointed out in 1909 (reference 1) apparently by Lanchester, that a propeller in yaw develops a considerable side force. The basic analysis was published in 1918 by R. G. Harris (reference 2), who showed that a pitching moment arises as well. Glauert (references 3 and 4) extended the method to derive the other stability derivatives of a propeller.

Harris and Glauert expressed the forces and moments in terms of the thrust and torque coefficients for the unyawed propeller, which were presumably to be obtained experimentally. The analyses did not take into account certain induction effects analogous to the downwash associated with a finite wing. It is noteworthy that with a semiempirical factor the Harris equation for side force does give good agreement with experiment. (See reference 5.) Pistolesi (reference 6) in 1928 considered the induction effects but his treatment was restricted to an idealized particular case. Klingemann and Weinig (reference 7) in 1938 published an analysis neglecting the induction effects; the treatment appears almost identical with the account given in 1935 by Glauert in reference 4.

There have been several notable attempts to express the side force directly in terms of the shape of the blades. Bairstow (reference 8) presented a detailed analysis in 1919 that neglected the induction effects. Misztal (reference 9) published an investigation in 1932 that did not have this limitation and that is probably the most accurate up to the present. Misztal's result, however, is in a very complex form from the point of view of both practical computation and physical interpretation; there is, in addition, an inaccuracy in the omission of the effects of the additional apparent mass of the air disturbed by the sidewash of the slipstream.

Very recently Rumph, White, and Grumman (reference 10) published an analysis that relates the side force directly to the plan form in a very simple manner. Reference 10, however, (1) does not include the ordinary inflow in the analysis and (2) applies unsteady-lift theory in an improper manner to account for the induction effects. As a consequence of (1), the equations are badly in error at high slipstream velocities. As a consequence of (2), the equations fail to predict the substantial increase in side force that experiment shows is provided by dual rotation. The improper use of unsteady-lift theory consisted in using formulas that apply to the case of a finite airfoil with an essentially rectilinear wake. The vortex loops shed by the finite airfoil, which produce the interference flow, are distributed along this rectilinear wake.

The corresponding vortex loops shed by a propeller blade in yaw, however, lie along the helical path traversed by the blade. The interference flow is quite different from the flow for the case of a rectilinear wake. In fact, it can be shown that the vortex loops shed during the unsteady lift aline themselves in such a way as to produce an inflow antisymmetry. This antisymmetry is one of the two induction effects that will be deduced in the present analysis from momentum considerations.

To sum up, there are available no analyses based on the blade shape that are sufficiently accurate over the whole range of propeller operating conditions and the analysis that is the most accurate is not in a satisfactorily simple form. For this reason a new method of analysis is presented that is an attempt at greater simplicity and accuracy. The present analysis shows that the fin analogy may be extended to the form of the side-force expression. The effective fin area may be taken as the projected side area[1] of the propeller and the effective aspect ratio is of the order of 8. This equivalent fin area may, with small error, be regarded as situated in the inflow at the propeller disk and subject to the corresponding augmented dynamic pressure. The variation with V/nD of the dynamic pressure at the propeller disk, for a fixed-pitch propeller, therefore accounts for most of the variation of side force with V/nD.

SYMBOLS

The formulas of the present report refer to a system of body axes. For single-rotating propellers, the origin is at the intersection of the axis of rotation and the plane of rotation; for dual-rotating propellers, the origin is on the axis of rotation halfway between the planes of rotation of the front and rear propellers. The X-axis is coincident with the axis of rotation and directed forward; the Y-axis is directed to the right and the Z-axis is directed downward. The symbols are defined as follows:

D propeller diameter
S' disk area $(\pi D^2/4)$
S wing area
R tip radius
r radius to any blade element
r_0 minimum radius at which shank blade sections develop lift (taken as $0.2R$)
x fraction of tip radius (r/R)
x_0 value of x corresponding to r_0 (r_0/R)
x_s ratio of spinner radius to tip radius
B number of blades
b blade section chord
c wing reference chord
μ relative blade section chord $\left(\dfrac{b}{b_{0.75R}} \text{ or } \dfrac{b/D}{(b/D)_{0.75R}}\right)$

$$\sigma' = B\left(\frac{b}{D}\right)_{0.75R}$$

[1] The projected side area is the area projected by the blades on a plane through the axis of rotation. For one or two blades this area varies with azimuth, but the average value is of concern here. The average projected side area is given to a close approximation by one-half the number of blades times the area projected by a single blade on a plane containing the blade center line and the axis of rotation.

σ solidity at $0.75R$ $\left(\dfrac{4}{3\pi}\sigma'\right)$
V free-stream velocity
a inflow factor $\left(\dfrac{\sqrt{1+\frac{8T_c}{\pi}}-1}{2}\right)$; in appendix B, speed of sound in free stream
a_n normal acceleration
g acceleration of gravity
V_a axial velocity at propeller disk $(V(1+a))$
V_t velocity component in direction of decreasing θ of relative wind at blade element $(2\pi nr$—Slipstream rotational velocity$)$
V_s slipstream velocity far behind propeller (in practice, 1 diam. or more) $(V(1+2a))$
q free-stream dynamic pressure $\left(\frac{1}{2}\rho V^2\right)$; also, angular velocity of pitching
$f_1(\phi)$ function defined in equation (1)
$t_1(\phi)$ function defined in equation (2)
$f(a)$ q-factor $\left(\dfrac{(1+a)[(1+a)+(1+2a)^2]}{1+(1+2a)^2}\right)$
$f_1(a) = \dfrac{2(1+2a)^2}{1+(1+2a)^2}$
n revolutions per second
J advance-diameter ratio (V/nD)
β blade angle to reference chord
β_0 blade angle to zero-lift chord
θ angle of blade relative to Y-axis measured in direction of rotation
ϕ effective helix angle including inflow and rotation $\left(\tan^{-1}\dfrac{V_a}{V_t}\right)$
ψ angle of yaw, radians
α effective angle of attack of blade element $(\beta_0-\phi)$
ϵ angle of sidewash in slipstream far behind propeller
ϵ' nominal induced angle of sidewash at propeller disk
$\bar{\epsilon}'$ effective average induced angle of sidewash at propeller disk
v_y sidewash velocity far behind propeller
C_L airplane lift coefficient
c_l blade section lift coefficient
c_{d_0} blade section profile-drag coefficient
c_{l_α} slope of blade section lift curve, per radian $(dc_l/d\alpha$; average value taken as $0.95\times2\pi)$
dF force component on a blade element in direction of decreasing θ (See fig. 1.)
T thrust
T_c thrust coefficient $(T/\rho V^2D^2)$
C_T thrust coefficient $(T/\rho n^2D^4)$
Q torque
Q_c torque coefficient $(Q/\rho V^2D^3)$
W weight of airplane
X, Y, Z forces directed along positive directions of X-, Y-, and Z-axes, respectively

L, M, N moments about X-, Y-, and Z-axes, respectively, in sense of right-handed screw; in appendix B and figure 9, M refers to the free-stream Mach number

M_e effective Mach number for propeller side force (See appendix B.)

A', B', C', D' functions defined in equations (4)

a', b', c', d' integrals defined by equations (21) and (30)

b_1, b_2 integrals defined by equations (31) and (32)

I_1 side-area index defined by equation (41) $\left(\frac{3\pi}{4}a'\right)$

I_2 integral defined by equation (42) $\left(\frac{3\pi}{4}b_1\right)$

I_3 integral defined by equation (43) $\left(\frac{3\pi}{4}d'\right)$

A' defined by equation (24) (zero for dual-rotating propellers)

A defined by equation (44) (zero for dual-rotating propellers)

m defined by equation (45)

k_1 correction factor defined by equation (34)

k_e sidewash factor defined by equation (35)

k_s spinner factor defined by equation (36)

K constant in equation for k_s

C_Y' side-force coefficient $\left(\frac{Y}{\frac{1}{2}\rho V^2 S'}\text{ or }\frac{8}{\pi}Y_c\right)$

C_m' pitching-moment coefficient $\left(\frac{M}{\frac{1}{2}\rho V^2 DS'}\text{ or }\frac{8}{\pi}M_c\right)$

$C_{Y'\psi}$ side-force derivative with respect to yaw $(\partial C_Y'/\partial\psi)$

$C_{m\psi}'$ pitching-moment derivative with respect to yaw $(\partial C_m'/\partial\psi)$

C_{Y_θ}' side-force derivative with respect to pitching $\left(\dfrac{\partial C_Y'}{\partial\left(\frac{qD}{2V}\right)}\right)$

C_{m_θ}' pitching-moment derivative with respect to pitching $\left(\dfrac{\partial C_m'}{\partial\left(\frac{qD}{2V}\right)}\right)$

S_p projected side area of propeller (See footnote 1.)

A aspect ratio

Subscripts:

$0.75R$ measured at $0.75R$ station $(x=0.75)$

c divided by $\rho V^2 D^2$ if a force, by $\rho V^2 D^3$ if a moment; designates quantities corrected for compressibility in appendix B and figure 9

e effective

k index that takes the values 1 to B to designate a particular propeller blade

max maximum

$stall$ at stall

A bar over a symbol denotes effective average value.

ANALYSIS

PROPELLER IN STEADY AXIAL FLIGHT

The section shown in figure 1 is part of a right-hand propeller blade moving to the right and advancing upward. The components of the relative wind are V_e and V_θ, where V_e is the axial velocity including the inflow and V_θ is the rotational velocity including the slipstream rotation. The force component in the direction of decreasing θ is:

$$dF=dL\sin\phi+dD\cos\phi$$

$$=\frac{\rho}{2}V_e^2 b\ dr\left(\frac{c_l\sin\phi+c_{d_0}\cos\phi}{\sin^2\phi}\right)$$

$$=\frac{\rho}{2}V_e^2 b\ dr[f_1(\phi)] \tag{1}$$

and the contribution to the thrust is

$$dT=dL\cos\phi-dD\sin\phi$$

$$=\frac{\rho}{2}V_e^2 b\ dr\left(\frac{c_l\cos\phi-c_{d_0}\sin\phi}{\sin^2\phi}\right)$$

$$=\frac{\rho}{2}V_e^2 b\ dr[t_1(\phi)] \tag{2}$$

The equations may be divided by $\rho V^2 D^2$ to reduce the terms to nondimensional form. Inasmuch as $V_e=V(1+a)$, there results

$$dF_c=\frac{(1+a)^2}{4}\frac{b}{D}f_1(\phi)dx$$

$$dT_c=\frac{(1+a)^2}{4}\frac{b}{D}t_1(\phi)dx$$

where

$$dF_c=\frac{dF}{\rho V^2 D^2}$$
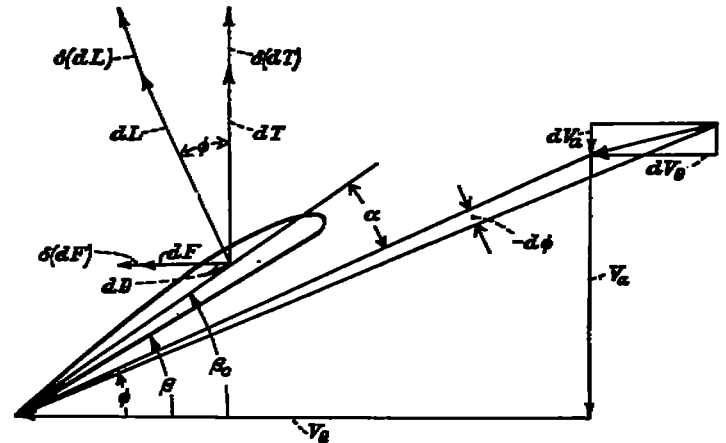
$$dT_c=\frac{dT}{\rho V^2 D^2}$$

and

$$x=\frac{r}{R}$$

FIGURE 1.—Vector relations at a blade element.

PROPELLER UNDER ALTERED FLIGHT CONDITIONS

Force components on blade element.—In equations (1) and (2) for dF and dT, V_a occurs explicitly in the factor V_a^2 and implicitly in ϕ and in terms depending on ϕ; V_θ occurs only implicitly in ϕ and in terms depending on ϕ. The relationship is $\phi = \tan^{-1}\frac{V_a}{V_\theta}$, which can be seen in figure 1. By partial differentiation, therefore, the increments in dF and dT due to any small changes whatsoever in V_θ and V_a are, for fixed blade angle,

$$\delta(dF) = \frac{\partial(dF)}{\partial\phi}\frac{\partial\phi}{\partial V_\theta}dV_\theta + \left[\frac{\partial(dF)}{\partial V_a} + \frac{\partial(dF)}{\partial\phi}\frac{\partial\phi}{\partial V_a}\right]dV_a$$

and a similar expression for $\delta(dT)$. The substitution of equations (1) and (2) gives, when put in nondimensional form,

$$\delta(dF_c) = \frac{(1+a)^2}{4}\frac{b}{D}dx\left[dV_\theta\frac{\partial\phi}{\partial V_\theta}\frac{\partial f_1}{\partial\phi} + dV_a\left(\frac{2f_1}{V_a} + \frac{\partial\phi}{\partial V_a}\frac{\partial f_1}{\partial\phi}\right)\right]$$

$$\delta(dT_c) = \frac{(1+a)^2}{4}\frac{b}{D}dx\left[dV_\theta\frac{\partial\phi}{\partial V_\theta}\frac{\partial t_1}{\partial\phi} + dV_a\left(\frac{2t_1}{V_a} + \frac{\partial\phi}{\partial V_a}\frac{\partial t_1}{\partial\phi}\right)\right] \quad (3)$$

The following abbreviations are helpful:

$$\left.\begin{aligned}\frac{A'}{V_a} &= \frac{\partial\phi}{\partial V_\theta}\frac{\partial f_1}{\partial\phi}\\[4pt]\frac{B'}{V_a} &= \frac{2f_1}{V_a} + \frac{\partial\phi}{\partial V_a}\frac{\partial f_1}{\partial\phi}\\[4pt]\frac{C'}{V_a} &= \frac{\partial\phi}{\partial V_\theta}\frac{\partial t_1}{\partial\phi}\\[4pt]\frac{D'}{V_a} &= \frac{2t_1}{V_a} + \frac{\partial\phi}{\partial V_a}\frac{\partial t_1}{\partial\phi}\\[4pt]\mu &= \frac{b/D}{(b/D)_{0.75R}}\end{aligned}\right\} \quad (4)$$

where f_1 and t_1 are defined in equations (1) and (2), respectively. Equations (3) become

$$\left.\begin{aligned}\delta(dF_c) &= \frac{(1+a)^2}{4}\left(\frac{b}{D}\right)_{0.75R}\left(A'\frac{dV_\theta}{V_a} + B'\frac{dV_a}{V_a}\right)\mu\, dx\\[4pt]\delta(dT_c) &= \frac{(1+a)^2}{4}\left(\frac{b}{D}\right)_{0.75R}\left(C'\frac{dV_\theta}{V_a} + D'\frac{dV_a}{V_a}\right)\mu\, dx\end{aligned}\right\} \quad (5)$$

where all the factors are nondimensional.

Forces and moments experienced by complete propeller.—Equations (5) give the component-force increments due to altered flight conditions on an element of a single blade, divided by $\rho V^2 D^2$. The force and moment increments experienced by the complete propeller of B blades, with respect to the body axes shown in figure 2, may be written as

Forces:

$$X - T = \sum_{k=1}^{k=B}\int_{r_0}^{R}\delta(dT)_k \quad (6)$$

$$Y = \sum_{k=1}^{k=B}\int_{r_0}^{R}\delta(dF)_k\sin\theta_k \quad (7)$$

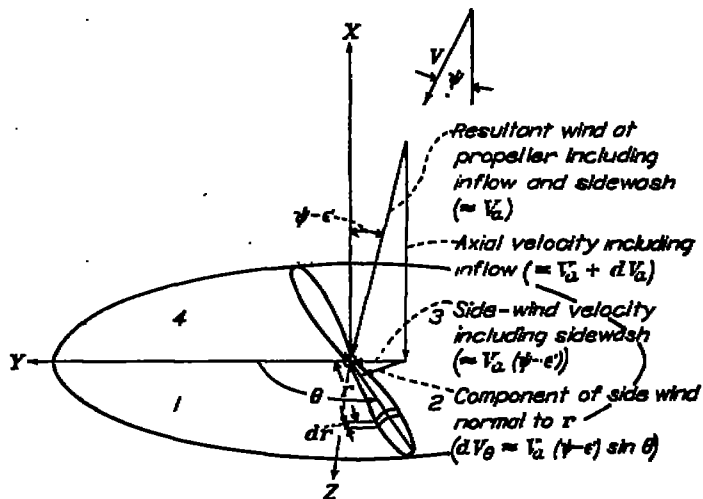$$Z = \sum_{k=1}^{k=B}\int_{r_0}^{R}\delta(dF)_k\cos\theta_k \quad (8)$$

FIGURE 2.—Vector relations for propeller in yaw.

Moments:

$$L - (-Q) = -\sum_{k=1}^{k=B}\int_{r_0}^{R}r\,\delta(dF)_k \quad (9)$$

$$M = \sum_{k=1}^{k=B}\int_{r_0}^{R}r\,\delta(dT)_k\sin\theta_k \quad (10)$$

$$N = -\sum_{k=1}^{k=B}\int_{r_0}^{R}r\,\delta(dT)_k\cos\theta_k \quad (11)$$

where the subscript k refers to the kth propeller blade. In order to obtain the nondimensional form X, Y, Z, and T are divided by $\rho V^2 D^2$ to give X_c, Y_c, Z_c, and T_c, and L, M, N, and Q are divided by $\rho V^2 D^3$ to give L_c, M_c, N_c, and Q_c. In the equations (6) to (11), $\delta(dF)_k$ becomes $\delta(dF_c)_k$, $\delta(dT)_k$ becomes $\delta(dT_c)_k$, and r becomes $\frac{r}{D} = \frac{x}{2}$. The limits of integration become x_0 to 1, where $x_0 = \frac{r_0}{R}$.

Stability derivatives of propeller.—The analysis up to this point has been of a general nature in that the formulas are applicable, for a fixed-pitch propeller, to any type of deviation from steady axial advance—that is, the formulas may be used to calculate all the stability derivatives of a fixed-pitch propeller. In addition, the formulas are applicable to those stability derivatives of a constant-speed propeller that are not associated with changes in blade angle. This restriction could be removed, however, by extending the analysis at the outset to include a term in $d\beta_0$.

A particular stability derivative can be obtained by determining and substituting in equations (5) the values of dV_θ/V_a and dV_a/V_a appropriate to the motion under consideration. For dual-rotating propellers equations (5) must be set up independently for both propeller sections with signs appropriate to the respective directions of rotation. Values of dV_θ/V_a and dV_a/V_a that are average for both sections are used for each section. Note that dV_θ is the change in the component of the effective relative wind acting on a blade in its plane of rotation and dV_θ must therefore include the effect of any changes induced by the motion in the rotational speed of the propeller relative to the airplane.

The possible unaccelerated motions of a propeller comprise flight (1) at a steady angle of yaw, (2) at a steady angle of pitch, (3) with an angular velocity of yaw, (4) with an angular velocity of pitch, (5) with an angular velocity of roll, (6) with an increment in forward speed, and any combination of these. It is clear from the symmetry of the propeller that motions (1) and (2) are similar and motions (3) and (4) are similar. Accordingly, of the six possible deviations of a propeller from a given mode of steady axial advance, only four are distinct. These four may be taken as angle of yaw ψ, angular velocity of pitch q, angular velocity of roll, and increment in forward velocity.

Glauert has shown in reference 3 that neither yawed flight nor flight with an angular velocity of pitch, when these disturbances are small, changes the torque on the propeller. Accordingly, neither mode will tend to change the rotational velocity, and derivatives with respect to yaw or angular velocity of pitch are independent of the rate of change of engine torque with engine revolutions. Furthermore, results for these derivatives obtained for a fixed-pitch propeller are equally applicable to a constant-speed propeller because the constant-speed mechanism is not brought into operation.

Both angular velocity of roll and increment in forward velocity clearly affect the torque of the propeller. The engine will attempt to alter its revolutions to attain an equilibrium value. If the propeller has fixed pitch, the adjustment will take place and its amount will depend upon the law of variation of engine torque with engine revolutions for the particular engine used. (See reference 3.) If the propeller is of the constant-speed type, the pitch-change mechanism will attempt to alter the blade pitch; the resulting change in aerodynamic torque opposes the change in revolutions. The fluctuations in rotational speed and the associated variations in aerodynamic torque and thrust of the propeller are then functionally related to the law of control of the pitch-change mechanism and the dynamics of its operation. (See reference 11.)

The present report will be limited to a study of the effects of yaw and of angular velocity of pitch. In the following sections dV_s/V_a and dV_a/V_a are evaluated for yawed motion.

PROPELLER IN YAW

Ratio dV_s/V_a for yawed motion.—The increment dV_s is the component parallel to V_s of a side-wind velocity computed as follows: The velocity V_a is regarded by analogy with wing theory as passing through the propeller disk at an angle $\psi - \epsilon'$ to the axis, where ψ is the angle of yaw and ϵ' may be termed the "induced sidewash angle" (fig. 2). The side-wind velocity, for small values of both ψ and ϵ', is accordingly $V_a(\psi - \epsilon')$.

The sidewash arises from the cross-wind forces. These forces are the cross-wind component of the thrust $T \sin \psi$ and of the side force known to be produced by yaw $Y \cos \psi$. (See fig. 3.) The analysis is restricted to small ψ; these components are then approximately $T\psi$ and Y.

If the sidewash velocity far behind the propeller is v_y, the induced sidewash at the propeller may be taken as $v_y/2$ by analogy with the relation between the induced downwash at a finite wing and the downwash far behind the wing. Note that 1 diameter may be considered "far" behind the propeller as regards the axial slipstream velocity; 95 percent of the final inflow velocity is attained at this distance.
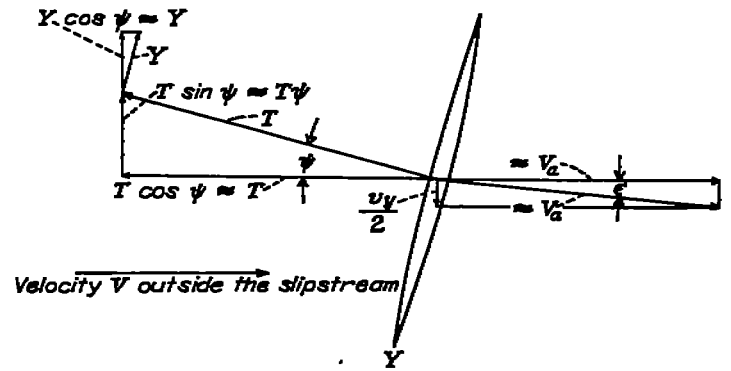

FIGURE 3.—Vector relations pertaining to the sidewash of a propeller in yaw. (All air velocities measured relative to propeller hub.)

As a first approximation, thrust and side force are assumed to be uniformly distributed over the propeller disk; corrections due to the actual distributions are investigated in appendix A. Under this assumption the momentum theory, supported qualitatively by vortex considerations, shows that the slipstream is deflected sidewise as a rigid cylinder. The sidewise motion induces a flow of air around the slipstream as in figure 4. The transverse momentum of this flow is, according to Munk (reference 12), equal to the transverse momentum of another cylinder of air having the same diameter as the slipstream at all points and moving sidewise with the same velocity as the slipstream boundary. Note that the air within the slipstream has a greater sidewise component of velocity than does the slipstream boundary. Far back of the propeller the ratio is $\frac{V_s}{V}=1+2a$. The time rate of change of the transverse momentum of the air flowing at free-stream velocity through this second cylinder should be included in setting up the momentum relations for the sidewash.
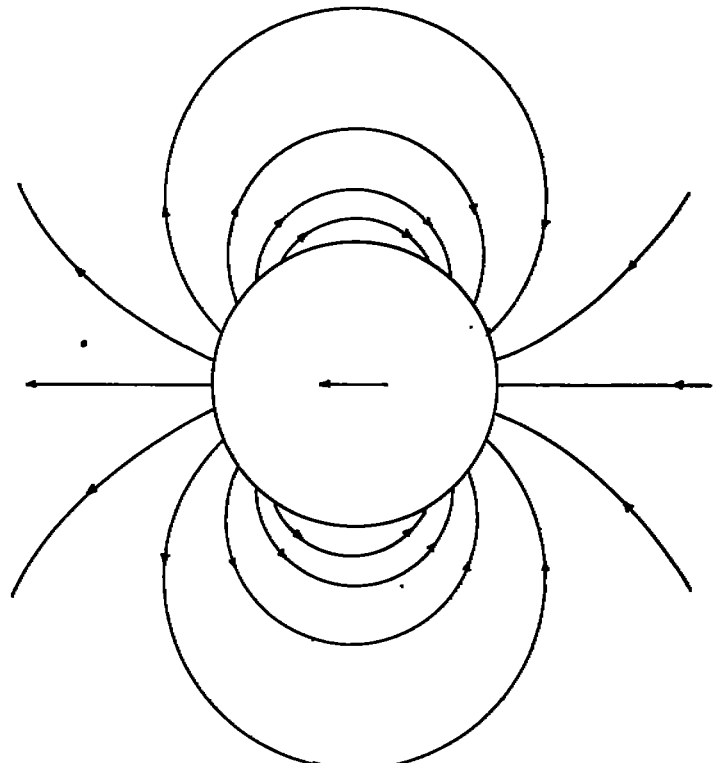

FIGURE 4.—Flow induced by the sidewise motion of an infinite cylinder in a fluid initially at rest.

By equating the cross-wind force to the total time rate of change of momentum,

$$T\psi + Y = \rho V_s \frac{\pi D^2}{4} v_y + \rho V \left(\frac{V_s}{V_s} \frac{\pi D^2}{4}\right)\left(\frac{V}{V_s} v_y\right)$$

to the first order in ψ, where the first term on the right is the contribution of the slipstream and the second term is the contribution of the air displaced by the slipstream. On dividing by $\rho V^2 D^2$ and using the relations $V_s = V(1+a)$ and $V_s = V(1+2a)$,

$$\frac{v_y 2}{V_s} = \frac{\frac{2}{\pi}(T_c\psi + Y_c)}{(1+a)^2\left[1+\frac{1}{(1+2a)^2}\right]} = \epsilon' \tag{12}$$

where ϵ' is the induced angle of sidewash at the propeller. Glauert (reference 4) deduces almost twice this value at small values of a by neglecting the reaction of the air displaced by the slipstream.

It was shown earlier that the effective side wind in the plane of the propeller is $V_s(\psi - \epsilon')$ and dV_s is the component parallel to V_s; that is,

$$dV_s = V_s(\psi - \epsilon')\sin\theta \tag{13}$$

The value of ϵ' from equation (12) may be introduced and the relation $\frac{2}{\pi}T_c = a(1+a)$, from simple momentum theory, may be used to eliminate T_c. There results

$$\frac{dV_s}{V_s} = \left[f(a)\psi - f_1(a)\frac{Y_c}{\pi}\right]\frac{\sin\theta}{(1+a)^2} \tag{13a}$$

where

$$f(a) = \frac{(1+a)[(1+a)+(1+2a)^2]}{1+(1+2a)^2} \tag{14}$$

and

$$f_1(a) = \frac{2(1+2a)^2}{1+(1+2a)^2} \tag{15}$$

Ratio dV_a/V_a for yawed motion.—As $V_a = V(1+a)$ for unyawed motion, the changes produced by yaw are

$$\frac{dV_a}{V_a} = \frac{dV}{V} + \frac{da}{1+a} \approx \frac{da}{1+a} \tag{16}$$

if dV/V, which is $\cos\psi - 1 \approx \frac{\psi^2}{2}$, is neglected as being of the second order in ψ.

In order to evaluate da, figure 2 is first considered. The component of the effective side wind in the direction opposite to the blade rotation is $dV_s = V_a(\psi - \epsilon')\sin\theta$. This component acts to increase the relative wind at the blade, and therefore the thrust, in quadrants 1 and 2; it acts to decrease the relative wind, and therefore the thrust, in quadrants 3 and 4. More exactly, the change in thrust due to the side wind is distributed sinusoidally in θ. It is clear that this incremental thrust distribution by its antisymmetry produces a pitching moment.

Momentum considerations require an increase in inflow in quadrants 1 and 2, where the thrust is increased, and a

decrease in inflow in quadrants 3 and 4, where the thrust is decreased. The variation should be sinusoidal in θ, and the assumption that the variation is directly proportional to the radius is sufficiently accurate for computing the effect on the side force. Such a representation is illustrated in figure 5.
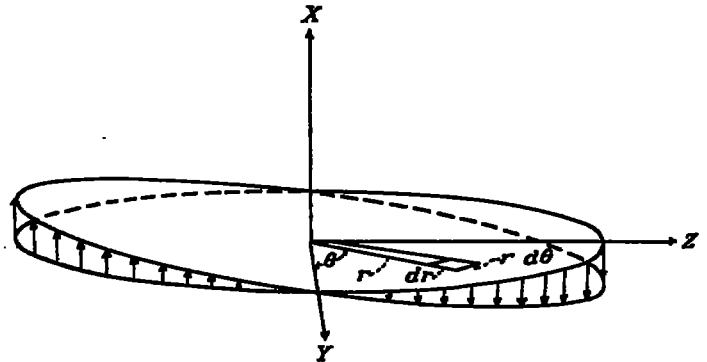

FIGURE 5.—Perspective view of three-dimensional graph of the assumed incremental inflow.

The analytical expression is

$$dv = V da$$
$$= kr\sin\theta \tag{17}$$

where k is a constant to be determined. Applying the momentum theory to evaluate the pitching moment M in terms of the inflow modifications produced by the pitching moment gives

$$M = \int_0^R \int_0^{2\pi} \rho V_a r\, d\theta\, dr\, r\sin\theta (2\, dv)$$

By substitution of the relation for dv,

$$M = 2k\rho V_a \int_0^R \int_0^{2\pi} r^3 \sin^2\theta\, d\theta\, dr$$

Upon integration,

$$k = \frac{16 V M_c}{(1+a)\pi R}$$

where

$$M_c = \frac{M}{\rho V^2 D^3}$$

but, by equations (16) and (17),

$$\frac{dV_a}{V_a} = \frac{da}{1+a}$$
$$= \frac{\frac{kr\sin\theta}{V}}{1+a}$$

or

$$\frac{dV_a}{V_a} = \frac{16 M_c x \sin\theta}{(1+a)^2\pi} \tag{18}$$

where

$$x = \frac{r}{R}$$

Summation over blade index k.—The component-velocity increments due to yaw have been obtained in the preceding two sections as

$$\frac{dT_e}{T_a}=\frac{1}{(1+a)^2}\left[f(a)-f_1(a)\frac{Y_e}{\tau}\right]\sin\theta_k \qquad (13a)$$

$$\frac{dT_e}{T_a}=\frac{1}{(1+a)^2}\left(\frac{16M_ex}{\tau}\right)\sin\theta_k \qquad (18)$$

where the subscript k has been added to refer to conditions at the kth propeller blade. These values of dT_e/V_a and dT_e/V_a may be substituted in equations (5) to yield values of $\delta(dF_e)$ and $\delta(dT_e)$. The values of $\delta(dF_e)$ and $\delta(dT_e)$ thus found may be inserted in equations (6) to (11), which give the several forces and moments the propeller might conceivably experience.

The summations over k indicated in equations (6) to (11) affect only the factors involving $\sin\theta_k$ and $\cos\theta_k$. The several factors are, upon evaluation,

$$\sum_{k=1}^{k=B}\sin\theta_k=\sum_{k=1}^{k=B}\sin\theta_k\cos\theta_k=0$$

If $B\geqq 3$,

$$\sum_{k=1}^{k=B}\sin^2\theta_k=\frac{B}{2}$$

If $B=2$ or 1,

$$\sum_{k=1}^{k=B}\sin^2\theta_k=\frac{B}{2}(1-\cos 2\theta_1)$$

but the average over θ is $B/2$.

The nonvanishing factor $\sum_{k=1}^{k=B}\sin^2\theta_k$ occurs only in equation (7) for the side force Y and in equation (10) for the pitching moment M. The other hypothetical forces and moments that might be produced by yaw are, accordingly, all zero.

When the relation

$$\sum_{k=1}^{k=B}\sin^2\theta_k=\frac{B}{2}$$

is used, equations (7) and (10) become in nondimensional form

$$Y_e=\frac{B}{8}\left(\frac{b}{D}\right)_{0.75R}\int_{x_1}^1\left\{\left[f(a)\psi-f_1(a)\frac{Y_e}{\tau}\right]A'+\frac{16}{\tau}M_eB'x\right\}\mu\,dx \qquad (19)$$

$$2M_e=\frac{B}{8}\left(\frac{b}{D}\right)_{0.75R}\int_{x_1}^1\left\{\left[f(a)\psi-f_1(a)\frac{Y_e}{\tau}\right]C'+\frac{16}{\tau}M_eD'x\right\}\mu x\,dx \qquad (20)$$

For simplicity the following additional abbreviations are introduced:

$$\sigma'=B\left(\frac{b}{D}\right)_{0.75R}.$$

$$a'=\frac{1}{\tau}\int_{x_e}^1\mu A'dx$$

$$b'=\frac{1}{\tau}\int_{x_e}^1\mu(-B')x\,dx \qquad (21)$$

$$c'=\frac{1}{\tau}\int_{x_e}^1\mu C'x\,dx$$

$$d'=\frac{1}{\tau}\int_{x_e}^1\mu(-D')x^2dx$$

where the signs have been chosen to make a', b', c', and d' positive quantities.

Solution for Y_e and M_e for single-rotating propellers.—With the preceding substitutions, equations (19) and (20) become

$$Y_e=\frac{\tau\sigma'}{8}\left\{\left[f(a)\psi-f_1(a)\frac{Y_e}{\tau}\right]a'-\frac{16}{\tau}M_eb'\right\}$$

$$2M_e=\frac{\tau\sigma'}{8}\left\{\left[f(a)\psi-f_1(a)\frac{Y_e}{\tau}\right]c'-\frac{16}{\tau}M_ed'\right\} \qquad (22)$$

These are simultaneous linear algebraic equations in Y_e and M_e. The solution for Y_e is, after simplification,

$$Y_e=\frac{\tau}{8}\psi\frac{f(a)\sigma'\left(a'-\frac{\sigma'b'c'}{1+\sigma'd'}\right)}{1+\sigma'\frac{f_1(a)}{8}\left(a'-\frac{\sigma'b'c'}{1+\sigma'd'}\right)}$$

which may be written in the form

$$Y_e=\frac{\tau}{8}\psi\frac{f(a)\sigma'a'}{\frac{a'}{a'-\Delta'}+\frac{f_1(a)}{8}\sigma'a'} \qquad (23)$$

where

$$\Delta'=\frac{\sigma'b'c'}{1+\sigma'd'} \qquad (24)$$

Numerical evaluation shows that the denominator of equation (23) does not differ greatly from unity; therefore, Y_e is roughly proportional to a'.

Similarly, the solution for M_e is

$$M_e=\frac{\tau}{2}\psi\frac{f(a)\sigma'c'}{[8+\sigma'f_1(a)a'](1+\sigma'd')-\sigma'^2f_1(a)b'c'}$$

which may be put in the form

$$M_e=\frac{\tau}{8}\psi\frac{f(a)m}{1+\frac{f_1(a)}{8}\sigma'(a'-\Delta')} \qquad (25)$$

where

$$m=\frac{\sigma'c'}{2(1+\sigma'd')} \qquad (26)$$

The relative magnitudes of the quantities are such that M_e is roughly proportional to c'.

Solution for Y_e and M_e for dual-rotating propellers.—The foregoing equations apply only to single-rotating propellers. With dual-rotating propellers the asymmetry of the disk loading, which for a single-rotating propeller produces the pitching moment due to yaw, is oppositely disposed over the front and rear sections. The resultant over-all disk loading, therefore, is almost symmetrical and gives rise to a negligible pitching moment—that is,

$$M_e\approx 0 \qquad (27)$$

The induction effects associated with the respective disk-loading asymmetries of the front and rear propeller sections very nearly cancel even though there is a finite separation between the two sections. This fact, which may be regarded as a consequence of the relation (27), is represented by putting $M_e=0$ in equation (22). The result is

$$Y_c = \frac{\pi}{8} \psi \frac{f(a)\sigma'a'}{1+\frac{1}{8}f_1(a)\sigma'a'} \tag{28}$$

This equation differs from equation (23), which applies to single rotation, in that unity replaces the larger quantity $\frac{a'}{a'-\Delta'}$ in the denominator. The side-force coefficient Y_c is therefore larger in the case of dual rotation. With data for conventional propellers, the increase averages about 18 percent and reaches 32 percent at low blade angles.

The increase in side force is due to the lack in the dual-rotating propeller of the asymmetric distribution of inflow velocity across the disk which, for the single-rotating propeller, is induced by the asymmetric disk loading. The inflow asymmetry is so disposed as to reduce the change in angle of attack due to yaw on all blade elements. The behavior is analogous to that of downwash in reducing the effective angle of attack of a finite wing.

The inflow asymmetry is not the only effect analogous to downwash in wing theory; the sidewash of the inflow is another such effect and serves to reduce the side force still further. Sidewash is, however, common to single- and dual-rotating propellers and affects both in the same way. An examination of the steps in the derivation shows that the term $\frac{1}{8}f_1(a)\sigma'a'$ in the denominator, the absence of which would increase the value of Y_c, is due to the sidewash.

Equations (23) to (28) give the stability derivatives of single- and dual-rotating propellers with respect to yaw, but the results are not yet in final form. There remain the evaluation of a', b', c', and d' and the introduction of a factor to account for the effect of a spinner and another factor to correct for the assumption of uniform loading of the side force over the propeller disk.

Explicit representation of a', b', c', and d'.—Equations (21) show a', b', c', and d' to be integrals involving the functions A', B', C', and D', respectively, which are defined in equations (4) in conjunction with equations (1) and (2). The quantities A', B', C', and D' are, upon evaluation,

$$\left.\begin{aligned}
A' &= c_{l_\alpha} \sin \phi + c_l \cos \phi \\
B' &= -[c_{l_\alpha} \cos \phi - c_l (\sin \phi + \csc \phi)] \\
C' &= c_{l_\alpha} \cos \phi - c_l (\sin \phi - 2 \csc \phi) \\
D' &= -\left(c_{l_\alpha} \frac{\cos^2 \phi}{\sin \phi} - c_l \cos \phi \right)
\end{aligned}\right\} \tag{29}$$

if terms in the coefficient of profile drag c_{d_0} are neglected as being small in comparison with the terms in c_{l_α}. The neglect of c_{d_0} is valid only for values of ϕ not too near 0° or 90°.

From figure 1, $\beta_0 = \phi + \alpha$. Then, for α in the unstalled range,

$$\sin \beta_0 = \sin \phi \cos \alpha + \sin \alpha \cos \phi$$
$$\approx \sin \phi + \alpha \cos \phi$$

and

$$c_{l_\alpha} \sin \beta_0 \approx c_{l_\alpha} \sin \phi + c_{l_\alpha} \alpha \cos \phi$$
$$= c_{l_\alpha} \sin \phi + c_l \cos \phi$$

the right-hand member of which is just A' in equation (29).

This relation provides the important result that, although both ϕ and c_l depend on the inflow, the slipstream rotation, and the value of V/nD, the function A' is independent of these quantities and depends solely on the geometrical blade angle β_0. This relationship leads directly to the interpretation, to be established presently, that the effective fin area of a propeller is essentially the projected side area.

The introduction of β_0 does not succeed in similarly eliminating ϕ and c_l from B', C', and D' but does result in a simplification in B' and C'. The summarized results are, to the first order in α, with D' left unchanged:

$$A' = c_{l_\alpha} \sin \beta_0$$
$$B' = -(c_{l_\alpha} \cos \beta_0 - c_l \csc \phi)$$
$$C' = c_{l_\alpha} \cos \beta_0 + 2c_l \csc \phi$$
$$D' = -\left(c_{l_\alpha} \frac{\cos^2 \phi}{\sin \phi} - c_l \cos \phi \right)$$

The integrals (21), in which A', B', C', and D' occur, must now be evaluated. Upon substitution,

$$\left.\begin{aligned}
a' &= \frac{c_{l_\alpha}}{\pi} \int_{x_0}^{1} \mu \sin \beta_0 \, dx \\
b' &= \frac{c_{l_\alpha}}{\pi} \int_{x_0}^{1} \mu x \cos \beta_0 \, dx - \frac{1}{\pi} \int_{x_0}^{1} \mu x c_l \csc \phi \, dx \\
c' &= \frac{c_{l_\alpha}}{\pi} \int_{x_0}^{1} \mu x \cos \beta_0 \, dx + \frac{2}{\pi} \int_{x_0}^{1} \mu x c_l \csc \phi \, dx \\
d' &= \frac{c_{l_\alpha}}{\pi} \int_{x_0}^{1} \frac{\mu x^2 \cos^2 \phi}{\sin \phi} \, dx - \frac{c_{l_\alpha}}{\pi} \int_{x_0}^{1} \mu x^2 \alpha \cos \phi \, dx
\end{aligned}\right\} \tag{30}$$

where

$$\mu = \frac{b}{b_{0.75R}}$$

and b is the blade width.

Evaluation of a', b', and c'.—The integral a' is already in its simplest form in equations (30), as is the first integral of b', which is identical with the first integral of c'. If the first integral of b' is defined as b_1,

$$\left.\begin{aligned}
b' &= b_1 - b_2 \\
c' &= b_1 + 2b_2
\end{aligned}\right\} \tag{31}$$

where

$$\left.\begin{aligned}
b_1 &= \frac{c_{l_\alpha}}{\pi} \int_{x_0}^{1} \mu x \cos \beta_0 \, dx \\
b_2 &= \frac{1}{\pi} \int_{x_0}^{1} \mu x c_l \csc \phi \, dx
\end{aligned}\right\} \tag{32}$$

In the attempt to evaluate b_2 it was found that, if the blade section coefficient of profile drag and the rotation of the slipstream are neglected, the thrust coefficient is

$$T_c = \frac{T}{\rho V^2 D^2}$$
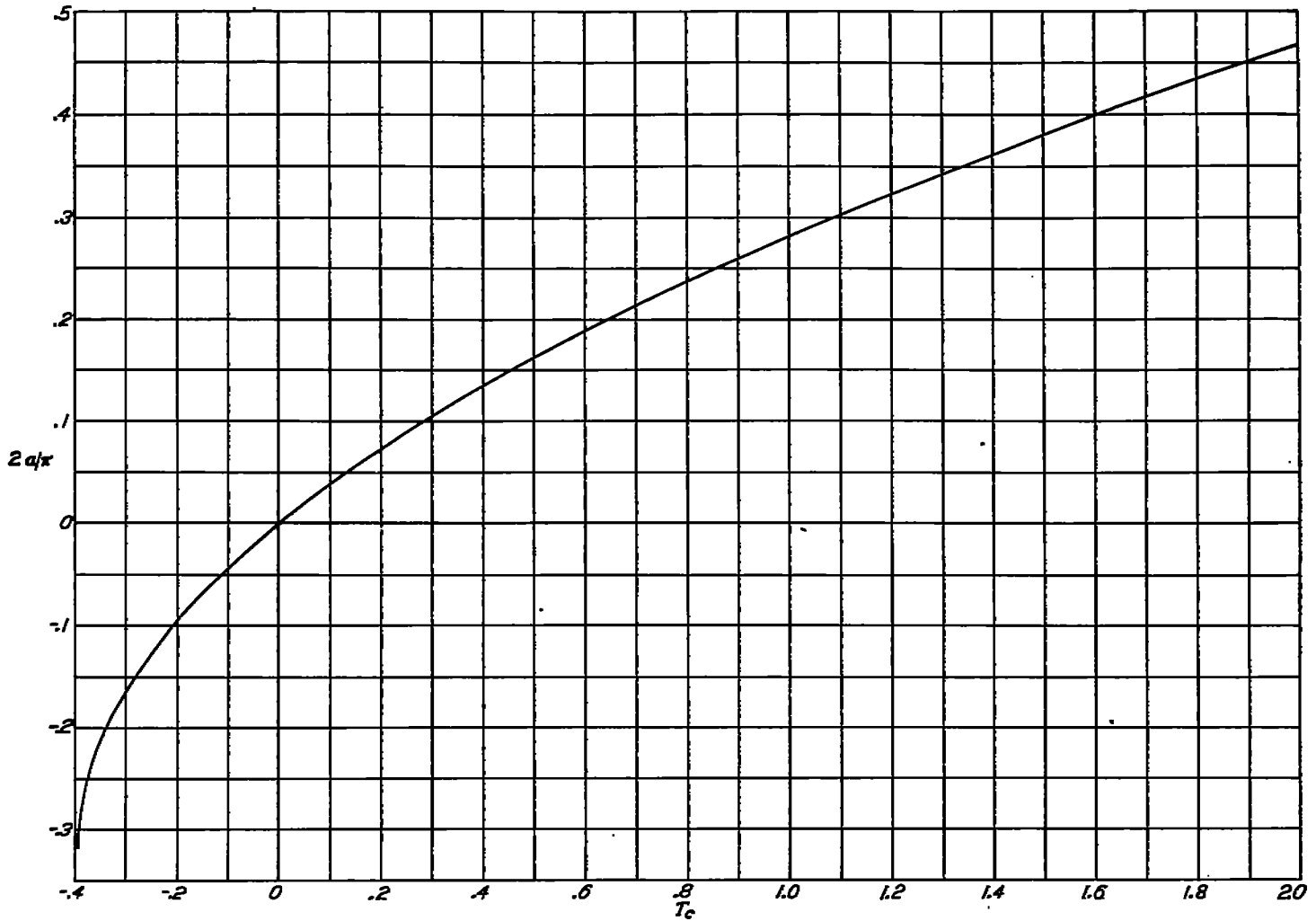$$= \int_{x_0}^{1} \frac{(1+a)\pi \sigma'}{4J} \mu x c_l \csc \phi \, dx$$

FIGURE 6.—Variation of $2a/\pi$ with T_c. $T_c = \frac{C_T}{(V/nD)^2}$.

where

$$J = \frac{V}{nD}$$

If an average value of $1+a$ over the disk is used, $1+a$ can be taken from under the integral sign, and

$$b_2 = \frac{J}{\sigma'} \frac{4T_c}{\pi^2(1+a)}$$

But, by the simple momentum theory,

$$\frac{2}{\pi} T_c = a(1+a)$$

Therefore,

$$b_2 = \frac{J}{\sigma'} \frac{2a}{\pi}$$

A graph of the variation of $2a/\pi$ with T_c is given in figure 6.

Approximate evaluation of d'.—The contribution of

$$d' = \frac{c_{l_\alpha}}{\pi} \int_{x_0}^{1} \mu x^2 \frac{\cos^2 \phi}{\sin \phi} \, dx - \frac{c_{l_\alpha}}{\pi} \int_{x_0}^{1} \mu x^2 \alpha \cos \phi \, dx$$

to V_c is small. It is found, by using the largest value which α may have without causing stalling of the blades (about

$\frac{1}{4}$ radian), that the second integral can be neglected, with the result that

$$d' = \frac{c_{l_\alpha}}{\pi} \int_{x_0}^{1} \mu x^2 \frac{\cos^2 \phi}{\sin \phi} \, dx$$

Note that ϕ involves the inflow velocity and the slipstream rotational velocity. These velocities, if assumed to be constant over the propeller disk, may easily be related to T_c and Q_c, respectively, from momentum considerations.

Curves of d' have been computed for a typical plan form (Hamilton Standard propeller 3155–6) and are presented in figure 7. This chart makes use of an altered notation introduced later in the report; the ordinate is the quantity

$$I_s = \frac{3\pi}{4} d'$$

and a parameter is the solidity at $0.75R$,

$$\sigma = \frac{4B}{3\pi} \left(\frac{b}{D} \right)_{0.75R}$$

The abscissa is V/nD. The error in computed side force due to using this chart for plan forms other than the Hamilton Standard 3155–6 should be negligible. The chart is not sufficiently accurate, however, for precise computation of the pitching moment due to yaw.
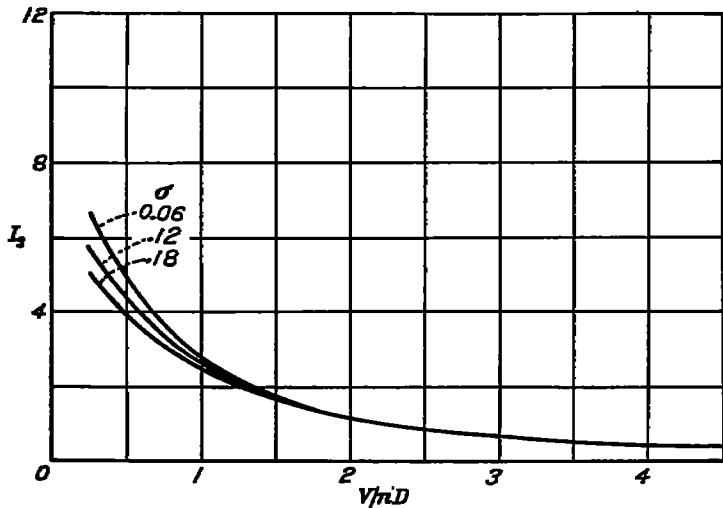
FIGURE 7.—Variation of L_s with V/nD and solidity. Approximate curves for blade-angle settings at which the blades are not stalled.

Correction for nonuniform distribution of side force.—
The induced sidewash angle ϵ' as calculated in the foregoing is based on the assumptions that the thrust and the side force are each uniformly distributed over the propeller disk. The error in effective average sidewash due to the assumption of uniform thrust distribution can be shown to be small; the error due to the assumption of uniform side-force distribution is appreciable. The effect of this error on the computed side force is small, but not negligible.

The side force is actually distributed over the propeller disk nearly as the product of the integrand of the most important term in the side-force expression a' and $\sin^2\theta$. The integrand of a' is proportional to the blade width times the sine of the blade angle, which tends to be greatest toward the blade roots due to the twist, and $\sin^2\theta$ has maximums at $\theta=90°$ and $270°$. The side force is therefore concentrated near the blade roots and along the Z-axis. In calculating an effective average of the part of ϵ' due to the side force, this distribution of the side force is taken into account by using in effect the integrand of a', which is $\mu \sin \beta$, times $\sin^2 \theta$ as a weight factor. The detailed treatment is given in appendix A. There is obtained for the effective average of the induced sidewash angle

$$\bar{\epsilon}'=\frac{\frac{2}{\pi}(T_c\psi+k_1Y_c)}{(1+a)^2\left[1+\frac{1}{(1+2a)^2}\right]} \tag{33}$$

where

$$k_1=\frac{\int_{x_s}^1 \frac{(\mu \sin \beta_0)^2}{x}dx}{\left(\int_{x_s}^1 \mu \sin \beta_0\, dx\right)^2} \tag{34}$$

is a correction factor derived in appendix A. If $\bar{\epsilon}'$ is inserted for ϵ' in the analysis for side force and pitching moment, the corrected forms of equations (23) and (25) are, respectively,

$$Y_c=\frac{\pi}{8}\psi \frac{f(a)\sigma'a'}{\frac{a'}{a'-\Delta'}+k_a\sigma'a'}$$

$$M_c=\frac{\pi}{8}\psi \frac{f(a)m}{1+k_a\sigma'(a'-\Delta')}$$

where the abbreviation

$$k_a=\frac{f_1(a)k_1}{8}$$

$$=f_1(a)\frac{\int_{x_s}^1 \frac{(\mu \sin \beta_0)^2}{x}\, dx}{8\left(\int_{x_s}^1 \mu \sin \beta_0\, dx\right)^2} \tag{35}$$

has been used. The factor k_a may be called the sidewash factor.

Correction for augmentative effect of spinner.—If the spinner-nacelle or spinner-fuselage combination has a fairly large fineness ratio, the circumferential component of the side wind is speeded up in passing around the blade shanks (fig. 8) by approximately the factor

$$1+K\left(\frac{x_s}{x}\right)^2$$

where

$$x_s=\frac{\text{Spinner radius}}{R}$$

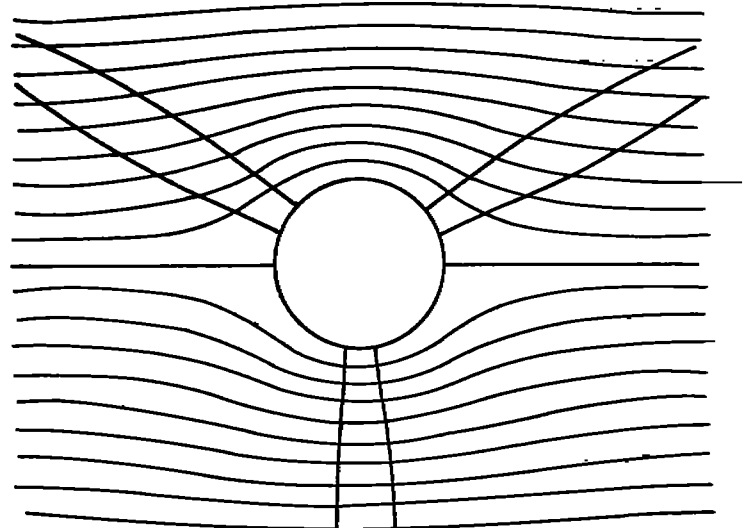K constant (1 for fineness ratio ∞; 0.90 for fineness ratio 6)

FIGURE 8.—Effect of spinner on the component of the flow in the plane of the propeller disk.

This local increase in side wind is equivalent to an increase in the angle of yaw ψ in the same ratio. Thus at radius xR the effective angle is

$$\psi_s(x)=\psi\left[1+K\left(\frac{x_s}{x}\right)^2\right]$$

The effective average yaw over the disk ψ_e is obtained from the consideration that dY_e is nearly proportional to the integrand $\mu \sin \beta$ of the dominant term a'. Approximately, therefore,

$$Y_e = k\psi \int_{x_t}^{1}\left[1+K\left(\frac{x_s}{x}\right)^2\right]\mu \sin \beta_0\, dx$$

$$= k\psi_e \int_{x_t}^{1}\mu \sin \beta_0\, dx$$

where k is a constant. Accordingly,

$$\frac{\psi_e}{\psi}=1+\frac{K\int_{x_t}^{1}\left(\frac{x_s}{x}\right)^2 \mu \sin \beta_0\, dx}{\int_{x_t}^{1}\mu \sin \beta_0\, dx}=k_s \qquad (36)$$

According to this result, if the propeller is equipped with a spinner, the previously given expressions for side force and pitching moment should be multiplied by the constant k_s, which may be termed the "spinner factor." The value of k_s is of the order of 1.14 and varies slightly with blade angle.

New definitions.—It is worth while to introduce certain new definitions at this point to put the final equations in better form. The original definitions were chosen solely with a view toward clarity in presenting the derivation. The principal change is the replacement of

$$\sigma'=B\left(\frac{b}{D}\right)_{0.75R}$$

which is proportional to the solidity at $0.75R$, by the actual solidity at $0.75R$

$$\sigma=\frac{4}{3\pi}\sigma'$$

$$=\frac{4B}{3\pi}\left(\frac{b}{D}\right)_{0.75R} \qquad (37)$$

This change entails replacing all the integrals occurring in the equation by $3\pi/4$ times the former values. Thus a' is replaced by I_1, b_1 by I_2, d' by I_3, and Δ' by Δ, where

$$I_1=\frac{3\pi}{4}a'$$

$$I_2=\frac{3\pi}{4}b_1$$

$$I_3=\frac{3\pi}{4}d'$$

$$\Delta=\frac{3\pi}{4}\Delta'$$

In addition, the following definitions are introduced:

$$C_Y'=\frac{Y}{qS'}$$

$$=\frac{8}{\pi}Y_c$$

$$C_{Y'\psi}=\frac{\partial C_Y'}{\partial \psi}$$

and

$$C_m'=\frac{M}{qDS'}$$

$$=\frac{8}{\pi}M_c$$

$$C_{m'\psi}=\frac{\partial C_m}{\partial \psi}$$

where the propeller disk area

$$S'=\frac{\pi D^2}{4}$$

The symbols C_Y' and C_m' have been so chosen in relation to the conventional side-force and pitching-moment coefficients of an airplane $C_{Y\psi}$ and $C_{m\psi}$ that conversion is obtained through the relations

$$C_{Y\psi}=\frac{\partial Y/\partial \psi}{qS}$$

$$=\frac{S'}{S}C_{Y'\psi}$$

$$C_{m\psi}=\frac{\partial M/\partial \psi}{qcS}$$

$$=\frac{S'}{S}\frac{D}{c}C_{m'\psi}$$

where S is the wing area and c is the wing reference chord. Note that in all the foregoing ψ is measured in radians.

Correction of side force for compressibility.—It is shown in appendix B that a first-order correction for compressibility is obtained by dividing the side force by $\sqrt{1-M_e^2}$, where M_e is related to the stream Mach number M and V/nD by the curve of figure 9. The correction is valid only below the critical Mach number for the propeller.

Summarized effects of yaw.—With the new definitions, the side-force derivative for a single-rotating propeller is

$$C_{Y'\psi}=\frac{\partial Y/\partial \psi}{qS'}$$

$$=-\frac{k_s f(a)\sigma I_1}{\frac{I_1}{I_1-\Delta}+k_e\sigma I_1} \qquad (38)$$

and the side-force derivative for a dual-rotating propeller is

$$C_{Y'\psi}=\frac{\partial Y/\partial \psi}{qS'}$$

$$=\frac{k_s f(a)\sigma I_1}{1+k_e\sigma I_1} \qquad (39)$$

For a single-rotating propeller the pitching-moment derivative is

$$C_{m'\psi}=\frac{\partial M/\partial \psi}{qDS'}$$

$$=\frac{k_s f(a)m}{1+k_e\sigma(I_1-\Delta)} \qquad (40)$$

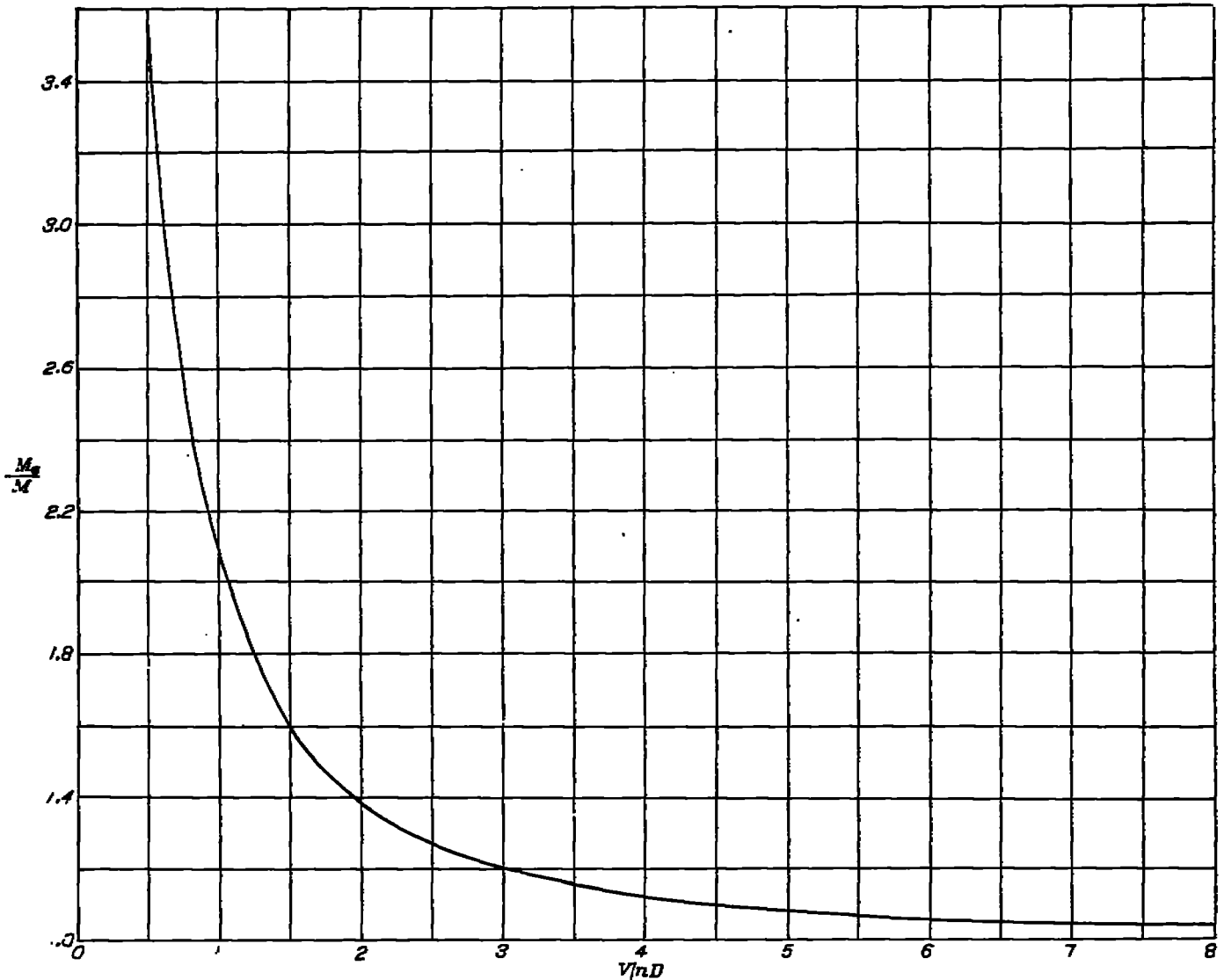and for a dual-rotating propeller the pitching-moment derivative is negligibly small.

FIGURE 9.—Variation of the ratio (Effective Mach number)/(Stream Mach number) with V/nD for use in relation $Cr'_{\psi}-\dfrac{Cr_{\psi}}{\sqrt{1-M_e^2}}$.

The side-force derivative may be corrected for compressibility by dividing by $\sqrt{1-M_e^2}$. The same correction may be applied to the pitching-moment derivative but with less accuracy.

The quantities involved are:

Spinner factor

$$k_s=1+\frac{K\int_{x_s}^{1}\left(\frac{x_s}{x}\right)^2 \mu \sin \beta_0\, dx}{\int_{x_c}^{1}\mu \sin \beta_0\, dx} \qquad (36)$$

Sidewash factor

$$k_s=f_1(a)\frac{\int_{x_s}^{1}\frac{\mu^2 \sin^2 \beta_0}{x}\, dx}{8\left(\int_{x_0}^{1}\mu \sin \beta_0\, dx\right)^2} \qquad (35)$$

where

$$f_1(a)=\frac{2(1+2a)^2}{1+(1+2a)^2}$$

Inflow factor

$$a=\frac{\sqrt{1+8\frac{T_c}{\pi}}-1}{2}$$

q-factor

$$f(a)=\frac{(1+a)[(1+a)+(1+2a)^2]}{1+(1+2a)^2} \qquad (14)$$

Solidity at $0.75R$

$$\sigma=\frac{4B}{3\pi}\left(\frac{b}{D}\right)_{0.75R} \qquad (37)$$

$$I_1=\frac{3}{4}c_{l_\alpha}\int_{x_0}^{1}\mu \sin \beta_0\, dx \qquad (41)$$

$$I_2=\frac{3}{4}c_{l_\alpha}\int_{x_0}^{1}\mu \cos \beta_0\, x\, dx \qquad (42)$$

$$I_3=\frac{3}{4}c_{l_\alpha}\int_{x_0}^{1}\mu \frac{\cos^2 \phi}{\sin \phi} x^2\, dx \qquad (43)$$

$$\Delta=\frac{\left(\sigma I_2-J\frac{2a}{\pi}\right)\left(\sigma I_1+2J\frac{2a}{\pi}\right)}{\sigma(1+\sigma I_3)} \qquad (44)$$

$$m=\frac{\sigma I_2+2J\frac{2a}{\pi}}{2(1+\sigma I_3)} \qquad (45)$$

and in equation (36), for a nacelle fineness ratio of 6, $K\approx0.90$ and, for a nacelle fineness ratio of ∞, $K\approx1.00$.

The charts of figures 6, 7, 10, and 11 are provided for determining $2a/\tau$, I_1, $f(a)$, and $f_1(a)$, respectively.

Required accuracy of k_s, k_e, and Δ.—To the degree in which comparison with existing experiments establishes the accuracy of the side-force formulas—about ±10 percent average error—it is sufficiently accurate to use the mean values 0.4 for k_e and, for the usual-size spinner ($x_s=0.16$), 1.14 for k_t. To the same accuracy, the terms in J may be omitted from Δ, and I_1 may be set equal to the average value 3, with the result that

$$\Delta\approx\frac{\sigma I_1^2}{1+3\sigma}$$

Availability of charts of side-force derivative.—In reference 13 is presented an extensive series of charts computed from equations (38) to (44) for two conventional propellers. The derivative $C_{Y'_\psi}$ is given as a function of V/nD for blade angles from 15° to 60° and for solidities from two blades to six blades, with single rotation and dual rotation. In reference 14 is presented a method of extrapolation whereby this set of charts may be used for determining $C_{Y'_\psi}$ for all conventional propellers without resort to the original equations (38) to (44).

Pitching-moment derivative.—By numerical evaluation of equation (40) the pitching moment of a single-rotating propeller in yaw is found to be of the order of the moment produced by a force equal to the side force acting at the end of a lever arm equal to the propeller radius. This moment is small and has heretofore been neglected in aircraft stability studies. Note that the effect is a cross-coupling between yaw and pitch.

The dual-rotating propeller develops no pitching moment.

PROPELLER SUBJECT TO ANGULAR VELOCITY OF PITCH

Ratio dV_t/V_a for angular velocity of pitch.—The angular velocity of pitch makes no direct contribution to the rotational velocity in the plane of the propeller disk V_t. It is known from Glauert's work (reference 3), however, that pitching gives rise to a side force and to a pitching moment. This side force induces a sidewash that affects V_t, as in the case of the yawed propeller. The change in V_t is accordingly the same as the induced part of the total change for yawed motion. This change is obtained by setting $\psi=0$ in equation (13a):

$$\frac{dV_t}{V_a}=-\frac{\sin\theta}{(1+a)^2}f_1(a)\frac{Y_e}{\tau} \tag{46}$$

where

$$f_1(a)=\frac{2(1+2a)^2}{1+(1+2a)^2} \tag{15}$$

Ratio dV_a/V_a for angular velocity of pitch.—The direct increment, due to pitching, in the axial velocity V_a is $qr\sin\theta$.

The induced increment due to the aforementioned pitching moment is, by equation (18),

$$\frac{V_a}{(1+a)^2}\frac{16M_c x}{\tau}\sin\theta$$

The total increment dV_a is the sum of the direct and the induced increments. Therefore

$$\frac{dV_a}{V_a}=\frac{\sin\theta}{(1+a)^2}\left[(1+a)\frac{qDx}{2V}+\frac{16M_c x}{\tau}\right] \tag{47}$$

Expressions for Y_e and M_c.—Upon introducing the equations (46) and (47), the equations that result here in place of equations (19) and (20) for the propeller in yaw are:

$$Y_e=\frac{B}{2}\frac{1}{4}\left(\frac{b}{D}\right)_{0.75R}\int_{x_0}^{1}\left\{\left[-f_1(a)\frac{Y_e}{\tau}\right]A'+\left[(1+a)\frac{qDx}{2V}+\frac{16M_c x}{\tau}\right]B'\right\}\mu\,dx$$

$$2M_c=\frac{B}{2}\frac{1}{4}\left(\frac{b}{D}\right)_{0.75R}\int_{x_0}^{1}\left\{\left[-f_1(a)\frac{Y_e}{\tau}\right]C'+\left[(1+a)\frac{qDx}{2V}+\frac{16M_c x}{\tau}\right]D'\right\}\mu x\,dx$$

$$\tag{48}$$

Solution for Y_e and M_c.—By using the abbreviations of equations (21), equations (48) become

$$Y_e=\frac{\pi\sigma'}{8}\left\{-f_1(a)\frac{Y_e}{\tau}a'-\left[(1+a)\frac{qD}{2V}+\frac{16M_c}{\tau}\right]b'\right\}$$

$$2M_c=\frac{\pi\sigma'}{8}\left\{-f_1(a)\frac{Y_e}{\tau}c'-\left[(1+a)\frac{qD}{2V}+\frac{16M_c}{\tau}\right]d'\right\}$$

which are simultaneous linear algebraic equations in Y_e and M_c. The solution for Y_e and M_c is, after simplification,

$$Y_e=-\frac{qD}{2V}(1+a)\frac{\pi}{8}\frac{\sigma I_2-J\frac{2a}{\tau}}{\left[1+\frac{f_1(a)}{8}\sigma(I_1-\Delta)\right](1+\sigma I_2)}$$

$$M_c=-\frac{qD}{2V}(1+a)\frac{\pi}{16}\frac{\sigma I_2\left(\frac{1+\frac{f_1(a)}{8}\sigma I_1}{1+\sigma I_2}\right)-\frac{f_1(a)}{8}\sigma\Delta}{1+\frac{f_1(a)}{8}\sigma(I_1-\Delta)}$$

Side-force derivative $C_{Y'_e}$ and pitching-moment derivative $C_{m'_e}$.—Side-force and pitching-moment derivatives may be defined as follows:

$$C_{Y'_q}=\frac{\partial Y/\partial\left(\frac{qD}{2V}\right)}{\frac{\rho}{2}V^2S'}$$

$$=-(1+a)\frac{\sigma I_2-J\frac{2a}{\tau}}{\left[1+\frac{f_1(a)}{8}\sigma(I_1-\Delta)\right](1+\sigma I_2)}$$

$$C_{m'_q}=\frac{\partial M/\partial\left(\frac{qD}{2V}\right)}{\frac{\rho}{2}V^2DS'}$$

$$=-\frac{1+a}{2}\frac{\sigma I_2\left(\frac{1+\frac{f_1(a)}{8}\sigma I_1}{1+\sigma I_2}\right)-\frac{f_1(a)}{8}\sigma\Delta}{1+\frac{f_1(a)}{8}\sigma(I_1-\Delta)}$$
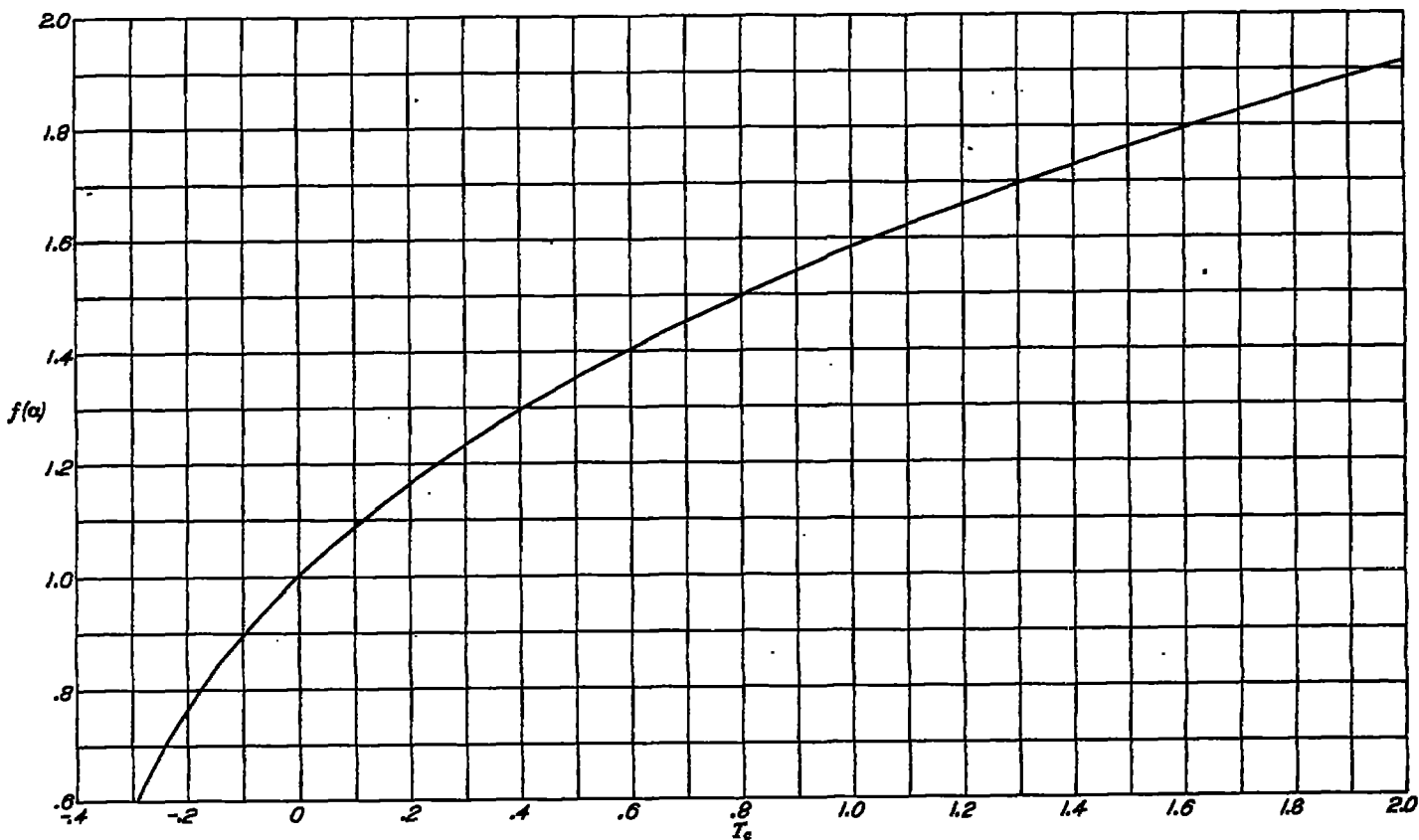
where

$$S'=\frac{\pi D^2}{4}$$

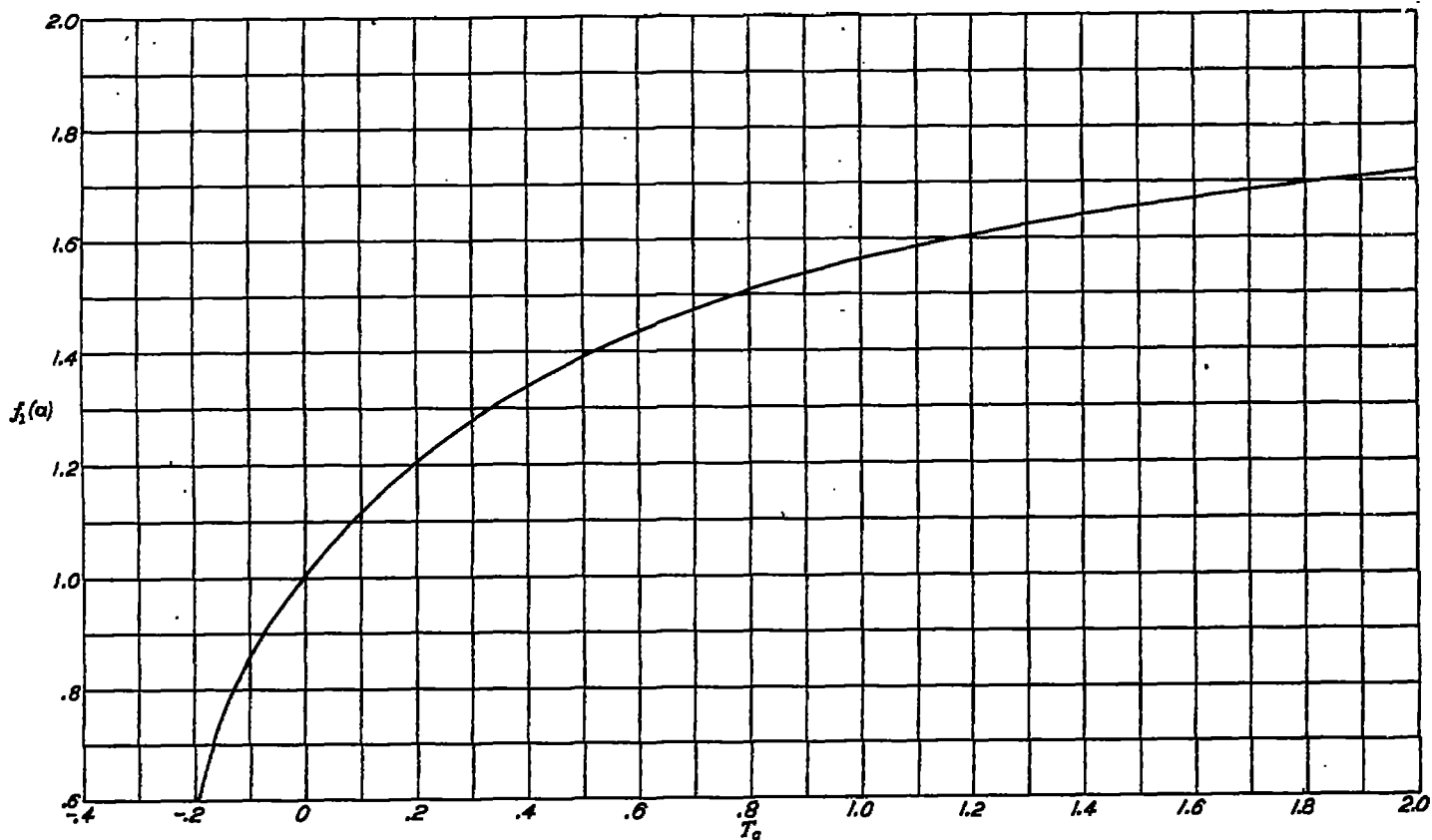FIGURE 10.—Variation of φ-factor $f(\alpha)$ with T_c.

FIGURE 11.—Variation of $f_1(\alpha)$ with T_c.

Rough approximations may be obtained by omitting the induction terms—that is, the terms due to sidewash and to inflow asymmetry. There result

$$
\left.\begin{array}{l}
C_{Y'_\epsilon} \approx -(1+a)\sigma I_1 \\
C_{m'_\epsilon} \approx -(1+a)\dfrac{\sigma I_3}{2}
\end{array}\right\} \qquad (49)
$$

Comparison of angle of yaw with angular velocity of pitch to produce same side force.—To the same rough approximation as equation (49),

$$
C_{Y'_\psi} \approx f(a)k_s\sigma I_1
$$

The ratio of ψ to $qD/2V$ to produce the same side force is therefore

$$
-\frac{\psi}{qD/2V} = -\frac{C_{Y'_\epsilon}}{C_{Y'_\psi}}
$$

$$
\approx \frac{(1+a)I_3}{f(a)k_sI_1}
$$

$$
\approx \frac{I_3}{k_sI_1} \qquad (50)
$$

This ratio is of the order of unity.

Maximum obtainable side force due to pitching.—The maximum side-force coefficient due to pitching occurs, for a given blade-angle setting, when $qD/2V$ is a maximum. Maximum $qD/2V$ in unstalled flight is determined by the maximum normal acceleration that the airplane can develop, which is determined by the maximum lift coefficient. The normal acceleration is

$$
a_n = qV
$$

from which

$$
\frac{qD}{2V} = \frac{a_nD}{2V^2} \qquad (51)
$$

At a given speed the maximum normal acceleration $a_{n_{max}}$ could be realized at the top of an inside loop. The relation is

$$
\frac{W}{g}a_{n_{max}} = \text{Downward lift} + \text{Weight}
$$

$$
= C_{L_{max}}S\frac{\rho}{2}V^2 + W
$$

or

$$
\frac{a_{n_{max}}}{V^2} = \left(\frac{\rho C_{L_{max}}}{2W/S} + \frac{1}{V^2}\right)g \qquad (52)
$$

The value of $a_{n_{max}}/V^2$ is greatest when V is least. If the discussion is limited for the present to the minimum speed for level flight V_{stall},

$$
\frac{\rho C_{L_{max}}}{2W/S} = \frac{1}{V_{stall}^2}
$$

From equation (52),

$$
\frac{a_{n_{max}}}{V^2} = \frac{2g}{V_{stall}^2}
$$

and therefore, from equation (51),

$$
\left(\frac{qD}{2V}\right)_{max} = \frac{gD}{V_{stall}^2}
$$

A practical upper limit to $(qD/2V)_{max}$ at the stalling speed would be afforded by a hypothetical fighter airplane having the following characteristics:

$$
V_{stall} = 75 \text{ mph}
$$
$$
= 110 \text{ fps}
$$
$$
D = 12 \text{ ft}
$$

Then

$$
\left(\frac{qD}{2V}\right)_{max} = \frac{32.2\times12}{(110)^2}
$$
$$
= 0.032
$$

By equation (50) the angle of yaw, in radians, that would provide the same side force is approximately

$$
\psi = -\frac{I_3}{k_sI_1}\left(\frac{qD}{2V}\right)_{max}
$$

If a minimum blade angle of 15° at stalling speed is assumed, the ratio I_3/k_sI_1 is 1.13 for the representative Hamilton Standard propeller 3155-6. Therefore, $(qD/2V)_{max}$ would be equivalent in producing side force to an angle of yaw

$$
\psi = -1.13\times0.032
$$
$$
= -0.036 \text{ radian or } -2.1°
$$

The resulting side force would be quite small.

Many times the preceding value of $(qD/2V)_{max}$ is obtainable during the spin, which involves wing stalling. If the spin is excluded from consideration, therefore, the general conclusion to be drawn from the example is that even in an extreme maneuver the side force due to rate of pitching is very small and in all ordinary maneuvers this side force is negligible.

Maximum obtainable pitching moment due to pitching.—The preceding data, when applied to the pitching moment due to pitching, indicate that the maximum obtainable pitching moment is of the order of the product of the propeller diameter and the maximum obtainable side force due to pitching. The general conclusion about the side force implies that the pitching moment due to pitching is small even in an extreme maneuver, with the exception of the spin, and in all ordinary maneuvers is negligible.

Forces due to angular velocity of yaw.—Angular velocities of yaw attain magnitudes of the same order as angular velocities of pitch. The forces on a propeller due to yawing are, like those due to pitching, negligible except in the spin.

PHYSICAL INTERPRETATION OF PROPELLER IN YAW

Concept of projected side area.—The area projected by a propeller blade on a plane through the axis of rotation and the axis of the blade is

$$
\int_{r_0}^{R} b \sin \beta_0 \, dr
$$

The average area projected by all the blades of a rotating propeller on any plane through the axis of rotation is the projected side area

$$S_p = \frac{B}{2}\int_{r_h}^{R} b \sin \beta_0 \, dr$$

where B is the number of blades. From this relation, it can be established that the product σI_1 may be expressed as

$$\sigma I_1 = c_{l_\alpha} \frac{S_p}{S'} \qquad (53)$$

where $S' = \frac{\pi D^2}{4}$ is the propeller disk area. Thus σI_1, which figures so prominently in the expressions for the side-force derivative $C_{Y'_\psi}$, is proportional to the projected side area of the propeller. In reference 13, I_1 is termed the "side-area index."

Effective fin area and aspect ratio.—Inasmuch as D^2/S_p is the aspect ratio A of the projected side area S_p, it is also true that

$$\sigma I_1 = \frac{c_{l_\alpha}}{2\pi} \frac{8}{A} \qquad (54)$$

Substitution of equation (53) in the numerator and equation (54) in the denominator of equation (39) gives for a dual-rotating propeller

$$\left.\begin{aligned} \frac{\partial Y/\partial\psi}{f(a)qS_p} &= k_s \frac{c_{l_\alpha}}{1 + k_s\left(\dfrac{c_{l_\alpha}}{2\pi}\right)\dfrac{8}{A}} \\[2ex] \frac{\partial Y/\partial\psi}{f(a)qS_p} &\approx k_s \frac{c_{l_\alpha}}{1 + \dfrac{3}{A}} \end{aligned}\right\} \qquad (55)$$

as $k_s \approx 0.4$ on the average and

$$\frac{c_{l_\alpha}}{2\pi} \approx 0.95$$

For comparison, the corresponding expression for an actual fin of the same area and aspect ratio, at which the local dynamic pressure is $f(a)q$, is

$$\frac{\partial Y/\partial\psi}{f(a)qS_p} = \frac{c_{l_\alpha}}{1 + \dfrac{2}{A}} \qquad (56)$$

when the lifting-line form of aspect-ratio correction is used. By omitting k_s, which merely accounts for the favorable interference between spinner and propeller, equation (55) can be written in the form of equation (56) by introducing an effective aspect ratio

$$A_e = \frac{A}{4k_s\dfrac{c_{l_\alpha}}{2\pi}}$$

$$\approx \frac{2}{3}A$$

It follows that a dual-rotating propeller in yaw acts like a fin of which the area is the projected side area of the propeller, the effective aspect ratio is approximately two-thirds the side-area aspect ratio, and the local dynamic pressure is $f(a)$ times the free-stream value. A single-rotating propeller may be shown to act similarly, but the effective aspect ratio is markedly less and is not so simply expressed. A mean effective aspect ratio for both single- and dual-rotating propellers is about 8.

Effective dynamic pressure.—By the definition of a, the expression $V(1+a)$ is the axial wind velocity at the propeller disk. Accordingly, $(1+a)^2q$ is the dynamic pressure at the propeller disk. The pressure $(1+a)^2q$ is only slightly greater than $f(a)q$, the effective dynamic pressure of equation (56). Thus the equivalent fin described in the preceding paragraph may with small error be regarded as situated in the inflow at the propeller disk and subject to the corresponding augmented dynamic pressure.

Comparison of side force of single- and dual-rotating propellers.—It has been pointed out in the discussion accompanying the derivation of Y_e and M_e for dual-rotating propellers in yaw that the dual-rotating propeller averages 18 percent more side force than the single-rotating propeller and that the increase reaches 32 percent at low blade angles. The detailed explanation is given in the same discussion. In brief, dual rotation eliminates certain induction effects associated with single rotation; the dual-rotating propeller acts as if it has a considerably higher aspect ratio and therefore develops more side force for the same solidity.

Magnitude of pitching moment.—It has been shown that yaw gives rise to zero pitching moment for a dual-rotating propeller and to a finite pitching moment, given by equation (40), for a single-rotating propeller. The numerical evaluation of equation (40) for typical cases shows that the pitching moment is of the order of the moment produced by a force equal to the side force, acting at the end of a lever arm equal to the propeller radius. This cross-coupling between pitch and yaw is small but possibly not negligible.

PROPELLERS IN PITCH

The results for propellers in yaw may be applied to propellers in pitch from considerations of symmetry. The normal-force derivative of a propeller with respect to pitch is equal to the side-force derivative of the same propeller with respect to yaw, and the yawing-moment derivative of a propeller with respect to pitch is equal to the negative of the pitching-moment derivative of the same propeller with respect to yaw. These relations are invalid when the propeller is in the upwash or downwash of a wing. (See reference 13.)

COMPARISON WITH EXPERIMENT

Experiments of Bramwell, Relf, and Bryant.—The experiments of Bramwell, Relf, and Bryant in 1914 with a four-blade model propeller in yaw (reference 15) are worth noting because the experimental arrangement was designed specifically for the problem. The balance was arranged to yaw
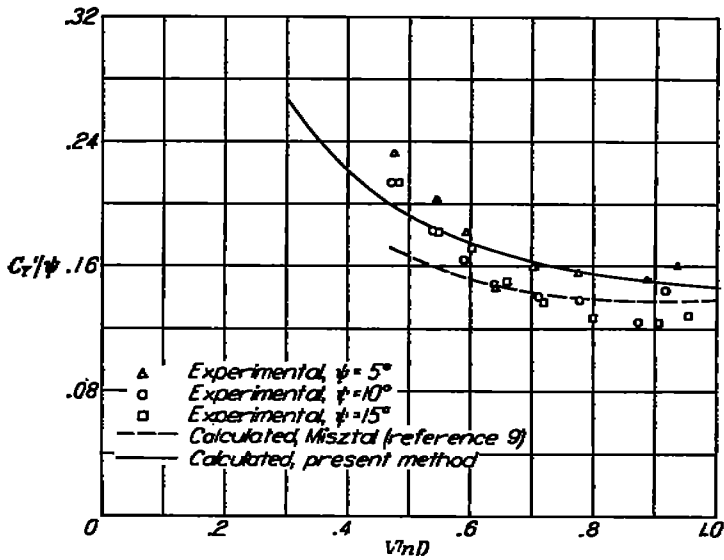
FIGURE 12.—Comparison of calculated curves of C_Y'/ψ with the experimental values of reference 15.

with the propeller and to measure the side force directly with respect to body axes. Tare readings were inherently small in comparison with the forces being measured. Tunnel speed was calibrated by comparison of thrust curves for the same propeller in the wind tunnel and on a whirling arm.

A calculated curve of C_Y'/ψ, which is the same as $C_{Y'\psi}$ for small values of ψ, is compared in figure 12 with the experimental values of reference 15. There is included for further comparison the theoretical curve calculated by Misztal (reference 9). The curve calculated from the formula of the present report appears to give somewhat better agreement than that of Misztal but the improvement is not conclusive. The principal objection to Misztal's formula remains the labor of its application rather than its defect in accuracy.

Experiments of Lesley, Worley, and Moy.—In the experiments of Lesley, Worley, and Moy reported in 1937 (reference 16), the nacelle was shielded from the air stream, with the result that only forces on the propeller blades were communicated to the balances. A 3-foot, two-blade propeller was used. Measurements were made of six components of the air forces on the propeller.

Calculated curves of C_Y'/ψ are compared with the experimental values of reference 16 for $\psi=10°$ in figure 13. Note that the original data of reference 16 were presented therein with respect to wind axes, and the data have been converted to the body axes of this report in the presentation of figure 13.

Experiments of Runckel.—The most complete experiments on yawed propellers [2]—the only published experiments on full-scale propellers—are those of Runckel (reference 17).

---

[2] The propellers of reference 17 were actually tested in pitch rather than in yaw but, inasmuch as pitch becomes yaw upon a 90° rotation of the axes, this conversion was made to keep the discussion consistent. In this connection, a vertical force due to pitch has herein been called a side force due to yaw.
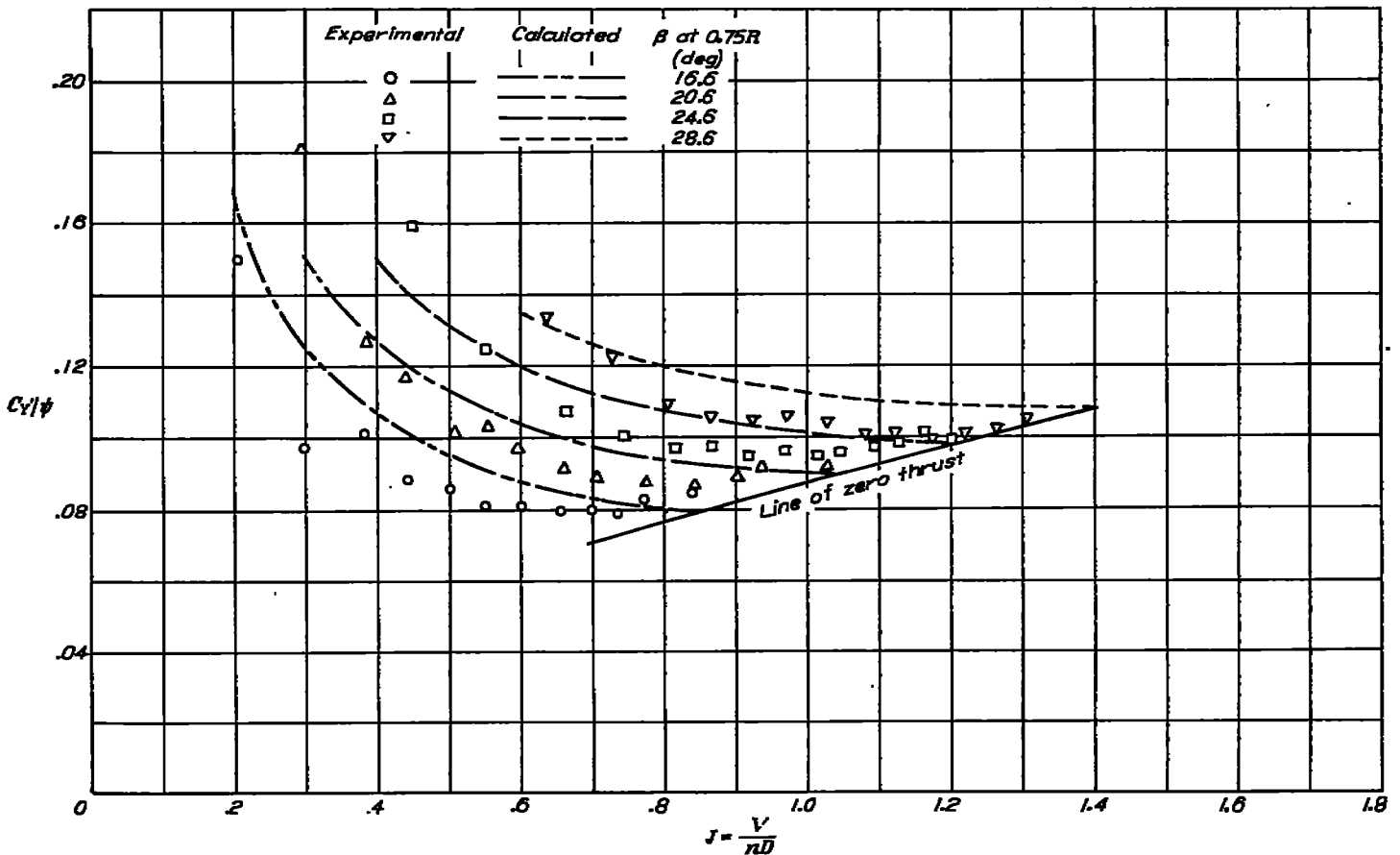

FIGURE 13.—Comparison of calculated and experimental values of C_Y'/ψ for two-blade model propeller. Curves are terminated, except for $\beta=16.6°$, at point where obvious stalling of blade occurs. Experimental data from reference 16 and converted from wind axes to body axes. $\psi=10°$
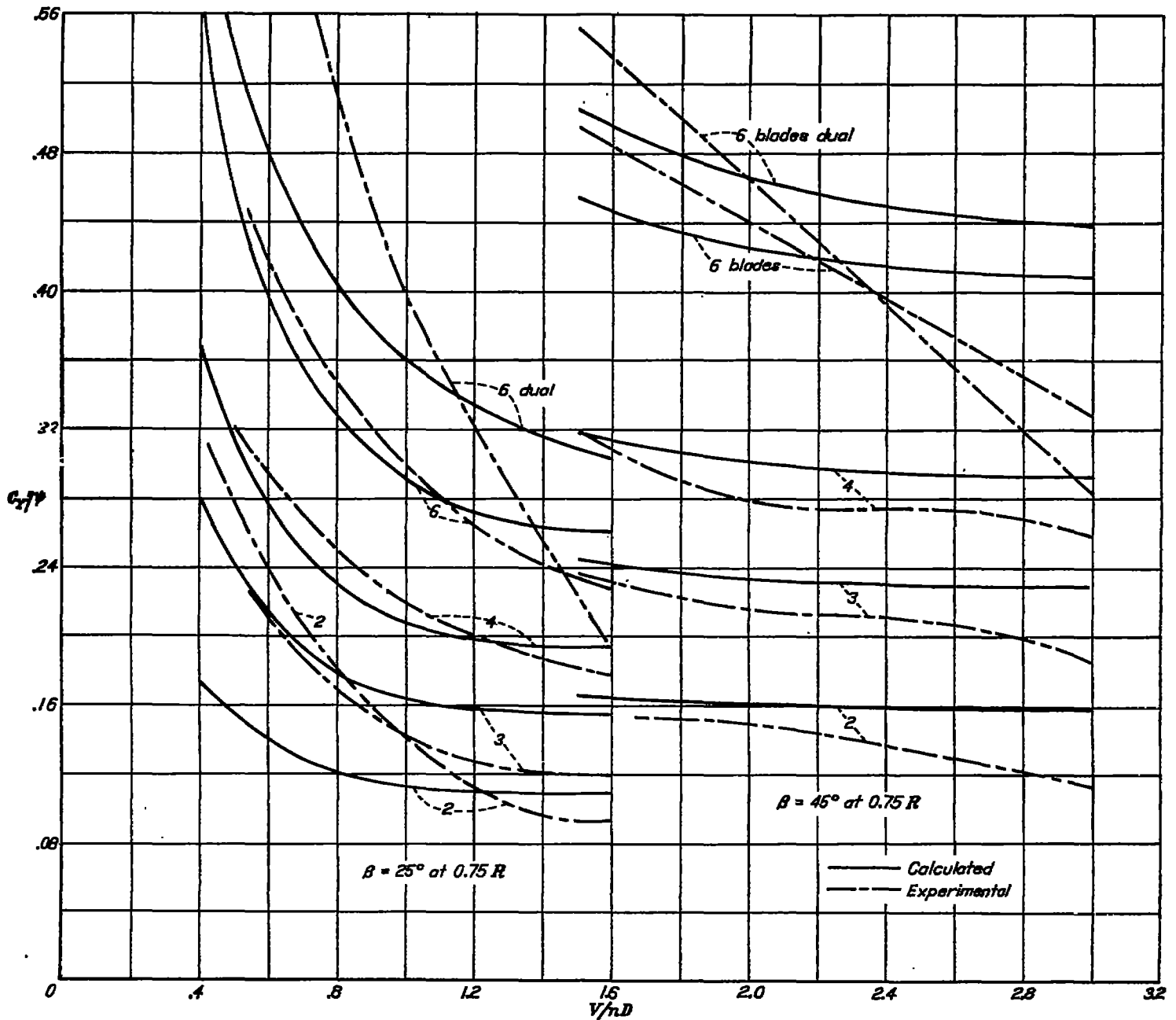
FIGURE 14.—Comparison of calculated curves of C_Y'/ψ with the faired experimental curves from reference 17 for 10° yaw. The original data with respect to pitch, with wind axes, have been converted to data with respect to yaw, with body axes.

Runckel tested single-rotating propellers of two, three, four, and six blades and a six-blade dual-rotating propeller. The diameter was 10 feet. An attempt was made to correct for the wind forces on the rather large unshielded nacelle by subtracting the forces and moments measured with zero yaw from the corresponding forces and moments measured with yaw at the same value of V/nD.

Calculated curves of C_Y'/ψ, including a spinner correction, are compared in figure 14 with the faired experimental curves from reference 17 for 10° yaw. In reference 17, as in reference 16, the original data were presented with respect to wind axes and the curves have been converted to the body axes

of this report in the presentation of figure 14. In figure 15 the unpublished experimental points for the single-rotating six-blade propeller are presented for comparison with the faired published curves as converted to body axes.

Accuracy.—From these several comparisons of the theory with experiment it appears that the average disagreement is slightly less than ±10 percent. This accuracy is of the order of that obtainable by the vortex theory for the un-inclined propeller when the number of blades is tacitly assumed to be infinite by the omission of the Goldstein correction for finite number of blades. The same assumption is made in the present analysis.
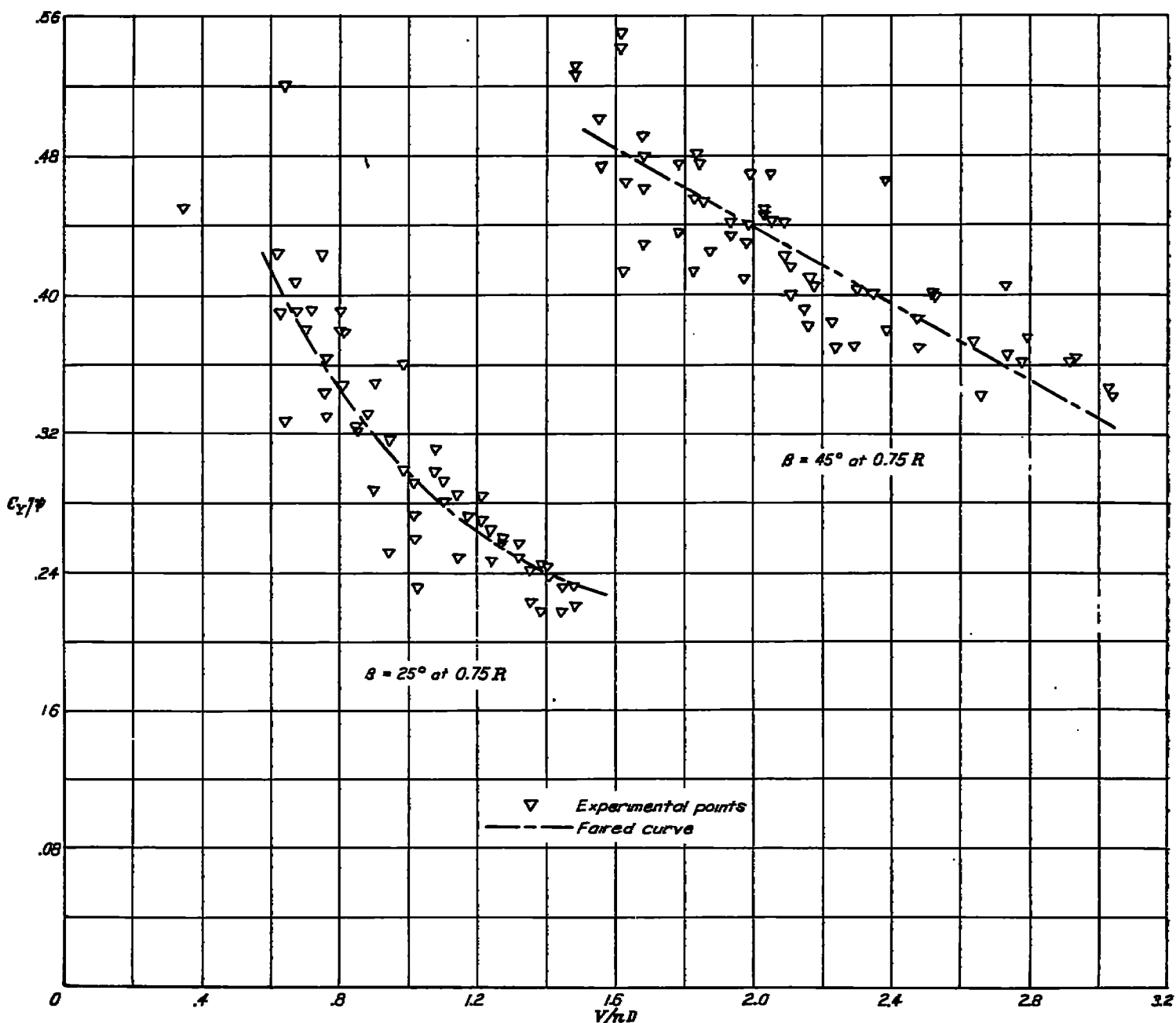
Figure 15.—Comparison of faired experimental curves of figure 14 for the six-blade single-rotating propeller with the unpublished experimental values referred to body axes.

CONCLUSIONS

The foregoing analysis of propellers in yaw and propellers subjected to an angular velocity of pitch permits the following conclusions:

1. A propeller in yaw acts like a fin of which the area is the projected side area of the propeller, the effective aspect ratio is of the order of 8, and the effective dynamic pressure is roughly that at the propeller disk as augmented by the inflow. The variation of the inflow velocity, for a fixed-pitch propeller, accounts for most of the variation of side force with advance-diameter ratio.

2. A dual-rotating propeller develops up to one-third more side force than a single-rotating propeller.

3. A yawed single-rotating propeller experiences a pitching moment as well as a side force. The pitching moment is of the order of the moment produced by a force equal to the side force, acting at the end of a lever arm equal to the propeller radius. This cross-coupling between pitch and yaw is small but possibly not negligible.

4. Propeller forces due to an angular velocity of pitch or yaw are negligibly small for the angular velocities that may be realized in maneuvers, with the exception of the spin.

APPENDIX A

DERIVATION OF SIDEWASH FACTOR k_s

If the assumption that the side force is uniformly distributed over the propeller disk is abandoned, it is necessary to proceed differently beyond equations (5) in deriving Y_c. For the purpose of obtaining an effective average induced sidewash, it is permissible to neglect the small term $B' \frac{dV_s}{V_s}$ in equation (5), which gives

$$\delta(dF_s) = \frac{(1+a)^2}{4}\left(\frac{b}{D}\right)_{0.75R}\frac{dV_s}{V_s}\mu A' dx \qquad (A1)$$

An equivalent differential relation for the time average side force, divided by $\rho V^2 D^2$, on an element of disk area $x\, d\theta\, dx$ may be substituted for the summation of equation (7), as

$$\frac{\partial^2 Y_c}{\partial x \partial \theta}dx\, d\theta = B\delta(dF_s)\sin\theta\frac{d\theta}{2\pi} \qquad (A2)$$

The fraction $\frac{dV_s}{V_s}$ has been shown to be given by

$$\frac{dV_s}{V_s} = (\psi - \epsilon')\sin\theta \qquad (13)$$

where ϵ' is the local induced angle of sidewash at the propeller disk. Combining equations (A1), (A2), and (13), using $A' = c_{l_\alpha}\sin\beta_0$, and assuming that $(1+a)^2$ is constant over the disk gives

$$\frac{dY_c}{d\theta} = \frac{c_{l_\alpha}\sigma'(1+a)^2\sin^2\theta}{8\pi}\int_{x_0}^{1}(\psi-\epsilon')\mu\sin\beta_0\, dx \qquad (A3)$$

from which

$$Y_c = \frac{c_{l_\alpha}\sigma'(1+a)^2}{8}\left(\psi\int_{x_0}^{1}\mu\sin\beta_0\, dx\right.$$
$$\left. -\frac{1}{\pi}\int_0^{2\pi}\int_{x_0}^{1}\epsilon'\sin^2\theta\,\mu\sin\beta_0\, dx\, d\theta\right)$$

An effective average value of ϵ' is obtained by defining

$$Y_c = \frac{c_{l_\alpha}\sigma'(1+a)^2}{8}\left[(\psi-\bar{\epsilon}')\int_{x_0}^{1}\mu\sin\beta_0\, dx\right] \qquad (A4)$$

from which the effective average angle of sidewash is

$$\bar{\epsilon}' = \frac{\frac{1}{\pi}\int_0^{2\pi}\int_{x_0}^{1}\epsilon'\sin^2\theta\,\mu\sin\beta_0\, dx\, d\theta}{\int_{x_0}^{1}\mu\sin\beta_0\, dx} \qquad (A5)$$

In this appendix the induced sidewash angle ϵ' is the local

212

value at the disk element $x\, dx\, d\theta$, not the average value used in the main text; ϵ' is composed of one part due to the side force ϵ'_Y and one part due to the cross-wind component of the thrust ϵ'_T. The effective averages are designated $\bar{\epsilon}'_Y$ and $\bar{\epsilon}'_T$. Then equations of the form of equation (A5) hold between $\bar{\epsilon}'_Y$ and ϵ'_Y and between $\bar{\epsilon}'_T$ and ϵ'_T.

The evaluation of $\bar{\epsilon}'_Y$ follows: The product $V_s\epsilon'_Y\sin\theta$, hereinafter called v_{θ_Y}, is a velocity component parallel to V_s but not necessarily in the same sense. In order to evaluate v_{θ_Y} for use in equation (A5), it is useful to define a quantity f such that $\frac{\partial^2 f}{x\,\partial x\partial\theta}x\, dx\, d\theta$ is the time average of the increment due to yaw of the peripheral force on an element of disk area $x\, dx\, d\theta$. Making the simplifying assumption that the peripheral force on an element of the propeller disk affects only the air flowing through that element and equating the peripheral force to the rate of change of peripheral momentum which this force produces far behind the propeller leads to the relation

$$\frac{\partial^2 f}{x\,\partial x\partial\theta}x\, dx\, d\theta = \rho V_s r\, dr\, d\theta\, 2v_{\theta_Y}+\rho V\left(\frac{V_s}{V_s}r\, dr\, d\theta\right)\left(\frac{V}{V_s}2v_{\theta_Y}\right)$$

(see derivation of equation (12)), or

$$\frac{v_{\theta_Y}}{V_s} = \frac{2\frac{\partial^2 f_c}{x\,\partial x\partial\theta}}{\left(\frac{V_s}{V}\right)^2\left[1+\left(\frac{V}{V_s}\right)^2\right]}$$

$$\frac{v_{\theta_Y}}{V_s} = \frac{2\frac{\partial^2 f_c}{x\,\partial x\partial\theta}}{(1+a)^2\left[1+\frac{1}{(1+2a)^2}\right]} \qquad (A6)$$

where

$$f_c = \frac{f}{\rho V^2 D^3}$$

$$V_s = V(1+a)$$

$$V_s = V(1+2a)$$

An alternative form of equation (A2) is

$$d^2 Y_c = \frac{\partial^2 f_c}{x\,\partial x\partial\theta}\sin\theta\, x\, dx\, d\theta$$

or

$$\frac{\partial^2 Y_c}{x\,\partial x\partial\theta} = \frac{\partial^2 f_c}{x\,\partial x\partial\theta}\sin\theta$$

In equation (A3) the fact that ϵ', which depends on θ, is small compared with ψ allows the approximate relation

$$\frac{\partial Y_c}{\partial \theta} = k \sin^2 \theta$$

where k is a constant. Integration establishes the value of k as Y_c/π; therefore

$$\frac{\partial Y_c}{\partial \theta} = \frac{Y_c \sin^2 \theta}{\pi}$$

$$\frac{\partial^2 Y_c}{\partial x \partial \theta} = \frac{\frac{\partial Y_c}{\partial x} \sin^2 \theta}{\pi}$$

By equation (A4),

$$\frac{\partial Y_c}{\partial x} = Y_c \frac{\mu \sin \beta_0}{\int_{x_0}^{1} \mu \sin \beta_0 \, dx}$$

Therefore

$$\frac{\partial^2 Y_c}{\partial x \partial \theta} = Y_c \frac{\mu \sin \beta_0}{\int_{x_0}^{1} \mu \sin \beta_0 \, dx} \frac{\sin^2 \theta}{\pi}$$

$$\frac{\partial^2 f_c}{x \, \partial x \partial \theta} = \frac{\sin \theta}{\pi} \frac{Y_c \, \mu \sin \beta_0}{x \int_{x_0}^{1} \mu \sin \beta_0 \, dx} \qquad (A7)$$

Equations (A6) and (A7) establish the value of v_{s_Y}/Y_c, which can be substituted for $\epsilon'_Y \sin \theta$ in equation (A5) as applied to $\bar{\epsilon}'_Y$ in place of $\bar{\epsilon}'$. This value is

$$\frac{v_{s_Y}}{Y_c} = \frac{2}{(1+a)^2 \left[1 + \frac{1}{(1+2a)^2} \right]} \frac{\sin \theta}{\pi} \frac{Y_c \, \mu \sin \beta_0}{x \int_{x_0}^{1} \mu \sin \beta_0 \, dx}$$

Therefore, substitution in (A5) as applied to $\bar{\epsilon}'_Y$ gives

$$\bar{\epsilon}'_Y = \frac{2Y_c \int_0^{2\pi} \int_{x_0}^{1} \sin^2 \theta \frac{(\mu \sin \beta_0)^2}{x} \, dx \, d\theta}{\pi^2 (1+a)^2 \left[1 + \frac{1}{(1+2a)^2} \right] \left(\int_{x_0}^{1} \mu \sin \beta_0 \, dx \right)^2}$$

The integration with respect to θ results in

$$\bar{\epsilon}'_Y = \frac{\frac{2}{\pi} Y_c}{(1+a)^2 \left[1 + \frac{1}{(1+2a)^2} \right]} \left[\frac{\int_{x_0}^{1} \frac{(\mu \sin \beta_0)^2}{x} \, dx}{\left(\int_{x_0}^{1} \mu \sin \beta_0 \, dx \right)^2} \right] \qquad (A8)$$

The part of ϵ' due to Y_c in equation (12), which is based on the assumption of uniform distribution of thrust and side force over the propeller disk, differs from the expression for $\bar{\epsilon}'_Y$ given by equation (A8) only in the absence of the factor

$$k_1 = \frac{\int_{x_0}^{1} \frac{(\mu \sin \beta_0)^2}{x} \, dx}{\left(\int_{x_0}^{1} \mu \sin \beta_0 \, dx \right)^2} \qquad (A9)$$

which is equation (34). An analysis for ϵ'_T similar to that for $\bar{\epsilon}'_Y$ results in a value that does not appreciably differ from the part of ϵ' due to T_c in equation (12); that is,

$$\bar{\epsilon}_T \approx \frac{\frac{2}{\pi} T_c \psi}{(1+a)^2 \left[1 + \frac{1}{(1+2a)^2} \right]}$$

Accordingly, the effective average induced angle of sidewash $\bar{\epsilon}'$, which equals $\bar{\epsilon}'_Y + \bar{\epsilon}'_T$, is given by

$$\bar{\epsilon}' = \frac{\frac{2}{\pi} (T_c \psi + k_1 Y_c)}{(1+a)^2 \left[1 + \frac{1}{(1+2a)^2} \right]}$$

which is equation (33). If $\bar{\epsilon}'$ is inserted for ϵ' in equation (12), the factor $f_1(a)/8$ in equations (23) and (25) is replaced by $\frac{f_1(a)}{8} k_1$. This is the quantity that has been called the sidewash factor k_s. With the value of k_1 inserted,

$$k_s = f_1(a) \frac{\int_{x_0}^{1} \frac{(\mu \sin \beta_0)^2}{x} \, dx}{8 \left(\int_{x_0}^{1} \mu \sin \beta_0 \, dx \right)^2} \qquad (35)$$

APPENDIX B

CORRECTION FOR COMPRESSIBILITY

The side-force derivative $C_{Y'_\psi}$ is very nearly proportional to the integral

$$I_I = \frac{3}{4} c_{l_\alpha} \int_{0.2}^{1} \mu \sin \beta_0 \, dx \tag{41}$$

To a first approximation the effect of compressibility is accounted for by replacing c_{l_α} by $c_{l_\alpha}/\sqrt{1-M_x^2}$, where M_x is the resultant speed of the blade section at x divided by the speed of sound in the free stream. If the subscript c is used to designate quantities corrected for compressibility effects,

$$I_{I_c} = \frac{3}{4} c_{l_\alpha} \int_{0.2}^{1} \frac{\mu \sin \beta_0 \, dx}{\sqrt{1-M_x^2}} \tag{B1}$$

A mean effective Mach number M_e defined by the relation

$$I_{I_c} = \frac{I_I}{\sqrt{1-M_e^2}} \tag{B2}$$

would also approximately satisfy the relation

$$C_{Y'_{\psi_c}} = \frac{C_{Y'_\psi}}{\sqrt{1-M_e^2}} \tag{B3}$$

Equation (B3) constitutes the desired correction of the side-force derivative for compressibility effects.

The determination of M_e proceeds as follows: By equations (41), (B1), and (B2),

$$\frac{1}{\sqrt{1-M_e^2}} = \frac{\int_{0.2}^{1} \frac{\mu \sin \beta_0 \, dx}{\sqrt{1-M_x^2}}}{\int_{0.2}^{1} \mu \sin \beta_0 \, dx}$$

For determining the ratio M_e/M it is sufficiently accurate to put

$$\frac{1}{\sqrt{1-M_e^2}} \approx 1 + \frac{M_e^2}{2} \tag{B4}$$

and

$$\frac{1}{\sqrt{1-M_x^2}} \approx 1 + \frac{M_x^2}{2} \tag{B5}$$

although approximation (B4) will not be applied to the final equation (B3). Then

$$M_e^2 = \frac{\int_{0.2}^{1} M_x^2 \, \mu \sin \beta_0 \, dx}{\int_{0.2}^{1} \mu \sin \beta_0 \, dx} \tag{B6}$$

By reference to figures 1 and 2, if inflow and rotation are neglected,

$$M_x^2 = \frac{V_e^2}{a^2 \sin^2 \phi}$$

$$= \frac{M^2}{\sin^2 \phi}$$

$$\approx M^2 \left[1 + \left(\frac{\pi x}{J} \right)^2 \right] \tag{B7}$$

where

a speed of sound in free stream
M free-stream Mach number

$$J = \frac{V}{nD}$$

$$x = \frac{r}{R}$$

The approximations $\mu = \text{Constant}$ and $\beta_0 = \phi$ are likewise adequate for the present purpose; therefore, as

$$\sin \phi \approx \frac{1}{\sqrt{1 + \left(\frac{\pi x}{J} \right)^2}}$$

equations (B6) and (B7) give

$$\left(\frac{M_e}{M} \right)^2 = \frac{\int_{0.2}^{1} \sqrt{1 + \left(\frac{\pi x}{J} \right)^2} \, dx}{\int_{0.2}^{1} \frac{dx}{\sqrt{1 + \left(\frac{\pi x}{J} \right)^2}}} \tag{B8}$$

Upon integration

$$\left(\frac{M_e}{M} \right)^2 = \frac{\frac{\sqrt{1+\lambda^2} - 0.2\sqrt{0.04+\lambda^2}}{\lambda^2} + \log_e \frac{1+\sqrt{1+\lambda^2}}{0.2+\sqrt{0.04+\lambda^2}}}{2 \log_e \frac{1+\sqrt{1+\lambda^2}}{0.2+\sqrt{0.04+\lambda^2}}} \tag{B9}$$

where

$$\lambda = \frac{J}{\pi}$$

$$= \frac{V/nD}{\pi}$$

Equation (B9) provides the desired relation between the effective Mach number M_e and the stream Mach number M for use in equation (B3). A graph of the variation of M_e/M with V/nD, computed from equation (B9), is given in figure 9.

Note that, in spite of the rapid rise of M_a/M with decreasing V/nD, for constant-speed propeller operation M_a decreases.

It may be noted that equations (B4) and (B5) are parabolic approximations to the Glauert compressibility factor $1/\sqrt{1-M^2}$. Equations (B6) to (B9) are, however, independent of the constants of the parabolic representation. Thus the validity of these equations is not restricted to the case of a variation of c_{l_α} with Mach number that follows the Glauert relation; the equations are valid for any variation that may be approximated in the region of interest by a parabola, such as

$$c_{l_{\alpha_c}}=(A+BM^2)c_{l_\alpha}$$

where A and B are constants.

The compressibility correction ceases to apply at Mach numbers above the critical Mach number for the propeller.

REFERENCES

1. Lanchester, F. W.: The Flying-Machine from an Engineering Standpoint. Constable & Co., Ltd. (London), 1917.

2. Harris, R. G.: Forces on a Propeller Due to Sideslip. R. & M. No. 427, British A. C. A., 1918.

3. Glauert, H.: The Stability Derivatives of an Airscrew. R. & M. No. 642, British A. C. A., 1919.

4. Glauert, H.: Airplane Propellers. Miscellaneous Airscrew Problems. Vol. IV of Aerodynamic Theory, div. L, ch. XII, secs. 5 and 6, W. F. Durand, ed., Julius Springer (Berlin), 1935, pp. 351-359.

5. Goett, Harry J., and Pass, H. R.: Effect of Propeller Operation on the Pitching Moments of Single-Engine Monoplanes. NACA ACR, May 1941.

*6. Pistolesi, E.: Nuove considerazioni sul problema dell'elica in un vento laterale. L'Aerotecnica, vol. VII, fasc. 3, March 1928, pp. 1-16.

7. Klingemann, G., and Weinig, F.: Die Kräfte und Momente der Luftschraube bei Schräganblasung und Flugzeugdrehung. Luftfahrtforschung, Bd. 15, Lfg. 4, April 6, 1938, pp. 206-218.

8. Bairstow, Leonard: Applied Aerodynamics. Second ed., Longmans, Green and Co., 1939.

9. Misztal, Franz: The Problem of the Propeller in Yaw with Special Reference to Airplane Stability. NACA TM No. 696, 1933.

10. Rumph, L. B., White, R. J., and Grummann, H. R.: Propeller Forces Due to Yaw and Their Effect on Airplane Stability. Jour. Aero. Sci., vol. 9, no. 12, Oct. 1942, pp. 465-470.

11. Weiss, Herbert K.: Dynamics of Constant-Speed Propellers. Jour. Aero. Sci., vol. 10, no. 2, Feb. 1943, p. 58.

12. Munk, Max M.: Fundamentals of Fluid Dynamics for Aircraft Designers. The Ronald Press Co., 1929, pp. 15-23.

13. Ribner, Herbert S.: Formulas for Propellers in Yaw and Charts of the Side-Force Derivative. NACA Rep. No. 819, 1945.

14. Ribner, Herbert S.: Proposal for a Propeller Side-Force Factor. NACA RB No. 3L02, 1943.

15. Bramwell, F. H., Relf, E. F., and Bryant, L. W.: Experiments on Model Propellers at the National Physical Laboratory. (II) Experiments to Determine the Lateral Force on a Propeller in a Side Wind. R. & M. No. 123, British A. C. A., 1914.

16. Lesley, E. P., Worley, George F., and Moy, Stanley: Air Propellers in Yaw. NACA Rep. No. 597, 1937.

17. Runckel, Jack F.: The Effect of Pitch on Force and Moment Characteristics of Full-Scale Propellers of Five Solidities. NACA ARR, June 1942.

*Translation available for reference or loan in Division of Research Information, National Advisory Committee for Aeronautics, Washington, D. C.